co2amp

Mikhail Polyanskiy

September 11, 2018

Contents

Chapter 1

General notes

1.1   Program capabilities

1. Ultrashort pulse amplification in CO_2 active medium

     Rotational numbers up to $J = 60$

     Regular, hot and sequence bands

     Isotopic CO_2

2. Molecular dynamics

     Realistic pumping

     Collisional relaxation processes

     Stimulated transitions

     Independent consideration of active medium regions at different elongations from the optical axis

3. Diffraction-based beam propagation

     Beam manipulation with common optical elements

     Arbitrary optical configurations

4. Linear dispersion and non-linear effects in optical materials

     Pulse chirping

     Kerr lensing

     Self-phase modulation

5. Advanced optics

     Chirped-pulse amplification

     Spectral filtering

     Trains of pulses

     Staging (program output as an input for the next stage stage)

6. User's interface

     Easy specification of parameters

     Graphical output

     Project save/recall

1.2   Availability and used software

The core of the `co2amp` code is written in `C` programming language; `C++` language is used for programming the user interface. Windows executables are built using the `MinGW` compiler (`http://www.mingw.org`). The entire code base of `co2amp` is published in the GitHub website (`https://github.com/polyanskiy/co2amp`) and is freely available for use, modification, and redistribution under the terms of the GNU General Public License (GPL) (`http://www.gnu.org/copyleft/gpl.html`). A binary package is provided in the form of a Windows installer that contains pre-compiled executables, documentation, and the source-code (all found in the installation directory after installation) at `https://github.com/polyanskiy/co2amp/releases/`. The user interface is built using a cross-platform library `QT` (`http://qt.io`) and thus should compile under other platforms supported by `QT` (MacOS, Linux). Third-party components used in the package (`gnuplot`, `7-zip`) also are freely available for multiple platforms (`http://www.gnuplot.info`, `http://www.7-zip.org`). The installer is built using the `Nullsoft Scriptable Install System` (NSIS, `http://nsis.sourceforge.net`), also an open-source software. Finally, the documentation is mostly written in L^ATEX (http://www.latex-project.org).

1.3   Acknowledgements

Viktor Platonenko from Moscow State University (Russia) provided a `Mathcad` code for pulse amplification in the CO_2 active medium that was used as the starting point for developing the `co2amp` program; Dr. Platonenko also offered valuable input in the early stages of the work.

Chapter 2

Program description

2.1   Basic concepts

The `co2amp` code allows simulating propagation of an ultrashort pulse through an arbitrary optical system that can include CO_2 amplifiers. Calculations of pulse amplification and fast molecular dynamics (stimulated transitions, and rotational relaxation) are undertaken in the time domain in the time-frame moving with the pulse("pulse time-frame"). Processes that are much slower than the duration of the pulse (e.g., discharge pumping, vibrational relaxation) are modeled separately in the laboratory time-frame.

The program input parameters include the characteristics of the initial pulse, the optical configuration, the composition of the active medium, the excitation parameters (e.g., discharge profile), and the number of nodes in the calculation grids for the time- (time-frame of the pulse) and space- (radial) coordinates. Axial symmetry is assumed at all times. The optical system can include multiple amplifiers provided that they have the same gas composition and pumping dynamics; sequential amplification in different amplifiers can be modeled using the staging option.

The temporal shape of the pulse and the beam profile at every element of the optical layout are saved and can be accessed in both graphical and tabulated-numerical representations. Complete pulse/beam information (complex field in every node of the time-space calculation grid) at the output of the system can also be saved and used as an input for another system (staging).

The user interface program supports the saving of all the inputs and outputs of the calculations as a single compressed file ('.co2' or '.co2x' extension). The difference between the two formats is that the files with extension ending with 'x' ("extended") include the complete information about the output field, and thus are suitable for staged calculations.

Fig. 2.1 shows the user interface of the `co2amp` program described in the following sections.

2.2   Input pulse and calculation grid

Unless the output of another simulation is used as an input (staged calculations), both the temporal shape of the input pulse and the profile of the input beam are assumed to be Gaussian; the pulse is assumed to be transform-limited (no initial chirping). The pulse energy, duration, central frequency, and the beam radius are entered in the corresponding fields in the input tab. The "Injection moment" parameter specifies the time-delay between the beginning of pumping of the active medium and injecting a pulse into the optical system. It is also possible to simulate the amplification of a train of identical equidistant pulses; in this case, the number of pulses in the train and time-delay between them must be specified.

The number of nodes in the calculation grid has to be specified for the radial coordinate and for the fast pulse time-frame (time-frame for the slow processes uses a fixed 1-ns step, and does not require a user input). The number of nodes always is a power of two that allows the use of Fast Fourier Transform (FFT) algorithms. Calculations with a larger number of nodes usually are more accurate but, on the other hand,
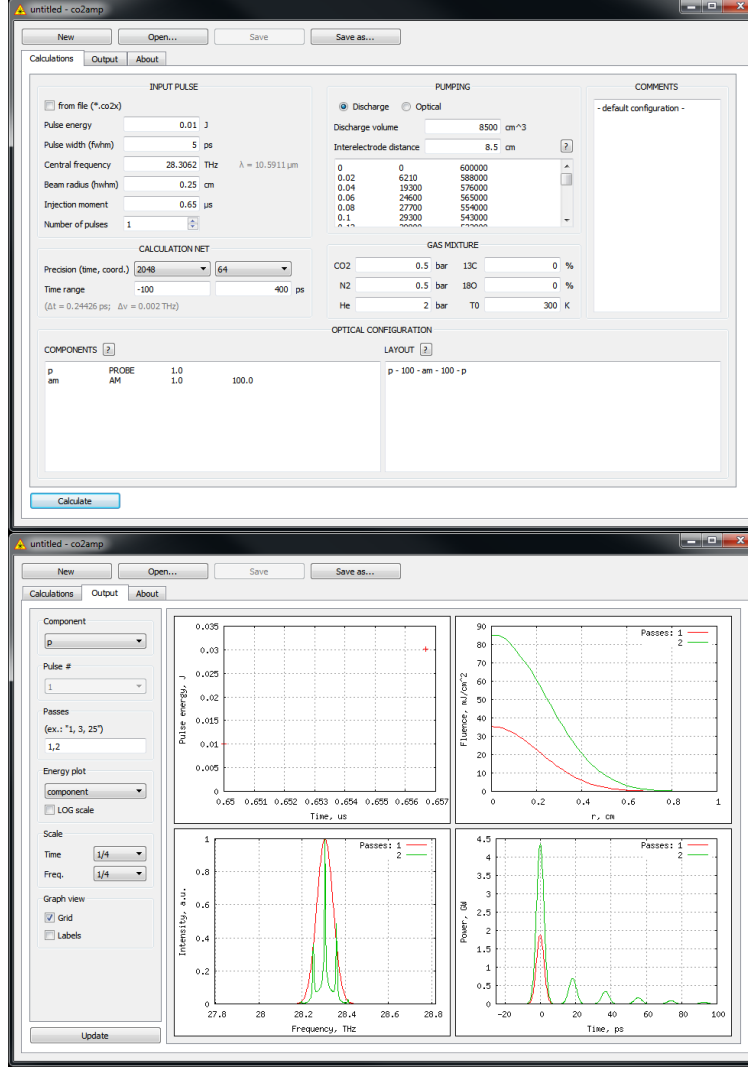
Figure 2.1: `co2amp` user interface: Input- (top) and output- (bottom) tabs.

take longer and require more computer memory (both calculation time and required memory are roughly proportional to the product of the number of nodes in the time and space grids). Therefore it is recommended to start running the simulation with a smaller number of nodes and then repeat it several times, each time with a denser grid. The absence of considerable change in the program's output with an increase in the number of nodes will indicate that the density of the grid is satisfactory.

Limits of the pulse time-frame ("time range") specify the time interval considered in the calculations. Initially, the pulse is centered at $t = 0$ and it tends to shift to longer delays upon amplification due to the limited response time of the medium and modulation of the spectrum. Thus, the optimum time range usually is asymmetric with a short negative part and a longer positive one. The time-step, $\Delta t = (t_{max} - t_{min})/(N_t - 1)$, where t_{max} and t_{min} define the time range and N_t is the number of nodes in the time grid, must be small enough to accurately describe the pulse profile at all stages of its propagation through the optical system. It also is important to remember that the time range and number of nodes in the time grid also define the range and step in the frequency domain: $\Delta\nu = 1/(t_{max} - t_{min})$ and $(\nu_{max} - \nu_{min}) = 1/\Delta t$. This means that the time range must be long enough to provide sufficient resolution in the frequency domain, while,

concurrently, the time step must be sufficiently short to provide a bandwidth that fits the entire spectral region of interest.

The maximum radial coordinate is defined separately for every element of the optical system, as detailed in the next section.

Identifying an appropriate calculation grid is very important for building an accurate model of an optical system. Putting an effort in this part of the simulation process will pay off with fast, reliable calculations.

2.3 Optical layout and beam propagation

The `co2amp` code uses a concept of optical surfaces similar to that employed in the ray-tracing algorithms. In this concept, the optical system is represented by a series of thin optical components (surfaces), each of which can alter the wave front. Between surfaces, beam propagates undisturbed. To specify the optical system the following must be done: 1) Describe all optical components, and 2) detail the locations of the components with respect to each other. In the `co2amp`'s user interface program, this is done by editing text in the two dedicated fields ("Components" and "Layout"). The format of these fields is described below.

2.3.1 Components

Each optical component is described in a separate line by several tab- or space-separated entries:

- Entry 1 '***ID***': An arbitrary user-defined alpha-numeric string for identifying the component;

- Entry 2 '***Type***': Type of the component; must be one of the types listed in Table 2.1;

- Entry 3 '***Field***': Maximum radial coordinate in centimeters to be considered in the simulations;

- Entry 4 '***Parameter 1***' and Entry 5 '***Parameter 2***': The meaning of these entries depends on the type of the component, as summarized in Table 2.1

The following example defines several components of 2.5-cm diameter: A probe surface, two 120-cm-long amplifier sections, a 5-cm-thick NaCl window, and an absorber for modeling 4% reflection losses:

```
p     PROBE        1.25
am1   AM           1.25   120
am2   AM           1.25   120
win   WINDOW       1.25   NaCl   5
att   ATTENUATOR   1.25   0.96
```

2.3.2 Layout

Optical configuration is specified as a sequence of the components identified by their ***ID***s. All components are separated by non-negative distances expressed in centimeters. Components and distances must be separated by spaces, tabs, line breaks, or dashes. The following is an example of an optical configuration that uses the components defined in the previous example:

```
p-0-att-0-win-0-att-100-am1-200-am2-100-att-0-win-0-att-0-p
```

This example defines the configuration shown in Fig. 2.2.

In this example, the beam propagates twice through the same amplifier. However, we consider this configuration as two identical but independent active volumes, `am1` and `am2`, because at each pass the beam interacts with a different zone of the active medium.

Table 2.1: Optical components

Type	Description	Parameter 1	Parameter 2
AM	Active medium	Length [cm]	-
PROBE	Passive surface, may be used as limiting aperture	-	-
MASK	Opaque circular screen	Radius [cm]	-
ATTENUATOR	Attenuator	Transmittance	-
LENS	Ideal lens (no spherical or chromatic aberrations)	Focal length [cm]	-
WINDOW	Transparent flat window (zero reflection and absorption losses)	Window material: KCl, NaCl, ZnSe, GaAs, CdTe, Ge, or Si (or with '-Brewster' modifier: KCl-Brewster, Si-Brewster etc.)	Thickness [cm]
STRETCHER	Stretcher or compressor	Pulse chirping [ps/THz] (positive for red-chirp)	-
BANDPASS	Band-pass filter	Band center [THz]	Bandwidth [THz]
APODIZER	Apodizing filter	Width of apodization as fraction of radial field $(0 \leq \alpha \leq 1)$	-
AIR	Air (model linear dispersion and n_2 related effects)	Humidity [%]	Length [cm]
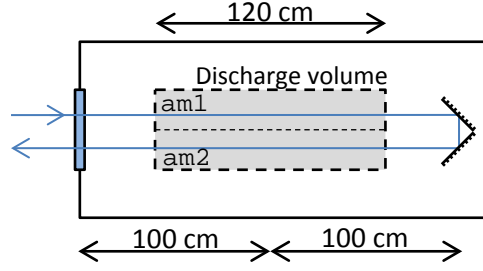
Figure 2.2: Example of optical configuration.

2.3.3 Beam propagation

When two components of an optical configuration are separated by a non-zero distance, beam propagation between them is simulated using the Huygens-Fresnel diffraction integral, assuming axial symmetry. Propagation is simulated separately for each moment of time from the time calculation grid.

The optical-surface model assumes that components of the optical layout are infinitely thin. For prolonged optical elements, propagation is calculated between the surfaces crossing the centers of the elements, and the beam is assumed to be collimated inside these elements. For instance, the following is the sequence of calculations for the previous example:

1. Interaction with the window (including reflection losses);

2. 100-cm propagation to the middle of the first pass through the amplifier (no amplification so far);

3. Amplification by a 120-cm amplifier section assuming that the beam is collimated;

4. 200-cm (100×2) propagation to the middle of the second pass through the active volume;

5. Amplification by the second 120-cm amplifier section, assuming that the beam is collimated;

6. 100-cm propagation to the window; and,

7. Interaction with the window.

Accuracy of the model can be improved if long elements (e.g. amplifiers) are divided into shorter sub-sections. This way we can more realistically simulate the variation of the profile of the beam during its propagation through the system. For instance, we can modify our example configuration as shown in Fig. 2.3.
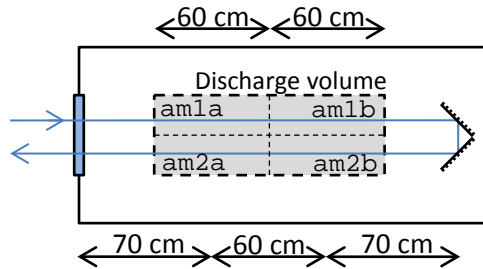
Figure 2.3: Example of a configuration modified for improved accuracy.

"Components" and "Layout" entries for the modified configuration are as follows:

Components:

```
p       PROBE       1.25
am1a    AM          1.25  60
am1b    AM          1.25  60
am2a    AM          1.25  60
am2b    AM          1.25  60
win     WINDOW      1.25  NaCl  5
abs     ATTENUATOR  1.25  0.96
```

Layout:

```
p-0-att-0-win-0-att-70-am1a-60-am1b-140-am2b-60-am2a-70-att-0-win-0-att-0-p
```

Population dynamics in all amplifier sections is modeled separately, and thus, by splitting a long amplifier into shorter sections we also obtain a more realistic model of the active medium.

2.4   Active medium and amplification

All the active medium sections used in a single simulation must have same gas composition and pumping conditions (staged simulations can be used for complex systems with two or more non-identical amplifiers). The composition (including isotopic enrichment of carbon dioxide) and the initial temperature of the active medium are specified in the "Gas mixture" fields of the input tab of the user interface.

Pumping by electric discharge is the primary pumping scheme of the co2amp code. For discharge pumping, the geometry of the discharge (discharge volume and the distance between electrodes) and its profile (tabulated values of discharge current expressed in amperes, and voltage in volts at time moments in microseconds) must be given. The pumping dynamics is calculated using a Boltzmann equation that takes into account elastic collisions between electrons and molecules, and the inelastic collisions with molecular rotational, vibrational and electronic excitations and ionization. The tabulated empirical values of corresponding cross-sections as functions of electron energy are used. The Boltzmann equation is solved repeatedly to assure our accurately describing the variation of pumping efficiency by the electric field changing during the discharge.

Initial support for optical pumping also is included. For optical pumping, the wavelength, the absorption cross-section, and the energy density of the pumping pulse must be provided.

2.5   Program output

The output of the program is given as a temporal pulse structure and its spectrum (both integrated across the beam) and beam profile (integrated on the duration of the pulse) at each element of the optical layout. The user can chose an optical component to display from the list of all the available components. If the selected component is used several times in the optical configuration, it also is possible to specify which passes through the component will be displayed. Also, the integral pulse energy can be provided either at every pass through a selected component, or at all passes through all components of the system's layout.

Output for the layout components of type AM (active medium) supplies additional information that includes gain, discharge profile, population dynamics, and the dynamics of the distribution of pumping energy (fractions of discharge energy going into the excitation of laser levels, excitation of molecular translations and ionization).

Chapter 3

Models

3.1 Molecular dynamics

Simulations of active medium pumping by electric discharge and vibrational relaxation are done following Karlov and Konev [15].

3.1.1 Pumping by electric discharge

Pumping is described by the Boltzmann equation in the following form [14, 20]:

$$-\frac{1}{3}\left(\frac{\mathcal{E}}{\mathcal{N}}\right)^2\frac{d}{du}\left[u\left(\sum_j y_j Q_{mj}(u)\right)^{-1}\frac{df(u)}{du}\right] \quad =$$

$$1.09\times10^{-3}\frac{d}{du}\left[u^2 f(u)\sum_j\frac{y_j}{M_j}Q_{mj}(u)\right] \quad + \quad \sum_{j=1,2} y_j C_j\frac{d}{du}(uf(u)) \quad + \quad 6By_2\frac{d}{du}(uQ(u)f)$$

$$+ \quad \sum_j y_j\sum_k(u+u_{jk})Q_{jk}(u+u_{jk})f(u+u_{jk}) \quad - \quad uf(u)\sum_j y_j\sum_k Q_{jk}(u) \tag{3.1}$$

where the left part describes the energy of electrons in the electric field, the first component of the sum of the right part represents energy transfer via elastic collisions between electrons and molecules, the second and third components describe collisions with molecular rotation excitation, and the two last components relate to inelastic collisions with transfer of the energy u_{jk} into vibrational and electronic excitations and ionization.

Electron energy u is expressed in eV;

Ratio of the electric field to the full molecular density, $\mathcal{E}/\mathcal{N}$, is expressed in units of 10^{-16} V·cm^2;

y_j are the relative molecule concentrations ($j = 1$ corresponds to CO_2, $j = 2$ to N_2 and $j = 3$ to He);

$M_1 = 44$, $M_2 = 28$, $M_3 = 4$ are the molar masses;

$C_1 = 8.2\times10^{-4}$ eV·Å^2 [12];

$C_2 = 5.06\times10^{-4}$ eV·Å^2 [10];

$B = 2.5\times10^{-4}$ eV is the N_2 rotational constant.

Numerical values of the cross-sections Q and the transferred energies u_{jk} are summarized in Appendix A

Equation 3.1 is solved numerically using the tridiagonal matrix algorithm. Distribution function $f(u)$ is then used in the following calculations.

The rate constant ω_{jk}, and the electron drift speeds v_d are defined as:

$$\omega_{jk}\left[\frac{\text{cm}^3}{\text{s}}\right] = 5.93 \times 10^{-9} \int\limits_0^\infty u Q_{jk}(u) f(u)\, du \tag{3.2}$$

$$v_d\left[\frac{\text{cm}}{\text{s}}\right] = -5.93 \times 10^7 \left(\frac{1}{3}\frac{\mathcal{E}}{\mathcal{N}}\right)\frac{df(u)}{du}\int\limits_0^\infty u\left(\sum_j y_j Q_{mj}(u)\right)^{-1} du \tag{3.3}$$

The fraction of electron energy transmitted via inelastic processes is defined as

$$z_{jk} = 10^{16}\frac{y_j u_{jk}\omega_{jk}}{\left(\frac{\mathcal{E}}{\mathcal{N}}\right)v_d} \tag{3.4}$$

The fraction of electron energy transmitted to translations and rotations are the following:

$$z_t = 5.93 \times 10^7 \frac{1.09 \times 10^{-3}\int\limits_0^\infty u^2\left(\sum_j \frac{y_j}{M_j}Q_{mj}(u)\right)f(u)\,du}{\left(\frac{\mathcal{E}}{\mathcal{N}}\right)v_d} \tag{3.5}$$

$$z_r = 5.93 \times 10^7 \frac{\sum\limits_{j=1,2} y_j C_j \int\limits_0^\infty u f(u)\,du + 6 y_2 B \int\limits_0^\infty u Q(u) f(u)\,du}{\left(\frac{\mathcal{E}}{\mathcal{N}}\right)v_d} \tag{3.6}$$

Finally, the distribution of the excitation energy is calculated using the following expressions:

$q_2 = \sum\limits_{k=1}^{6} z_{1k}$ - fraction of energy transferred to CO_2 symmetric stretch (ν_1) and bending (ν_2) modes;

$q_3 = z_{17}$ - fraction of energy transferred to CO_2 asymmetric stretch mode (ν_3);

$q_4 = \sum\limits_{k=1}^{8} z_{2k}$ - fraction of energy transferred to N_2 vibrations;

$q_T = z_t + z_r$ - fraction of energy transferred to translation and rotation;

$q_{ei} = \sum\limits_{k=9}^{15} z_{2k} + \sum\limits_{k=8}^{10} z_{1k}$ - fraction of energy spent on excitation of electronic levels and ionization.

3.1.2   Pumping and vibrational relaxation dynamics

A 3-temperature model is used for describing the vibrational dynamics of the active medium of CO_2 amplifiers. In this model, the following temperatures are used to describe the distribution of the energy between molecular vibrations:

T_2 – vibrational temperature of ν_1 and ν_2 vibrations of CO_2;

T_3 – vibrational temperature of the ν_3 vibration of CO_2;

T_4 – vibrational temperature of N_2.

Vibrational temperatures are related to the average numbers of quanta e_x in the corresponding vibrations as follows:

$$e_2 = \frac{2}{\exp(960/T_2) - 1}$$
$$e_3 = \frac{1}{\exp(3380/T_3) - 1} \tag{3.7}$$
$$e_4 = \frac{1}{\exp(3350/T_4) - 1}$$

"2" in the first equation is due to 2-fold degeneracy of the energy levels of the bend vibration.

The dynamics of pumping/relaxation is described by the following equations

$$\frac{de_4}{dt} = p_{e4} - r_a(e_4 - e_3)$$

$$\frac{de_3}{dt} = p_{e3} + r_c(e_4 - e_3) - r_3 f_3 \tag{3.8}$$

$$\frac{de_2}{dt} = f_2 \left(p_{e2} + 3r_3 f_3 - r_2(e_2 - e_{2T}) \right)$$

where

$$p_{e4} = 0.8 \times 10^{-3} \frac{q_4}{ny_2} W(t); \quad p_{e3} = 0.8 \times 10^{-3} \frac{q_3}{ny_1} W(t); \quad p_{e2} = 2.8 \times 10^{-3} \frac{q_2}{ny_1} W(t);$$

$$f_2 = \frac{2(1 + e_2)^2}{2 + 6e_2 + 3e_2{}^2}; \quad f_3 = e_3(1 + e_2/2)^3 - (1 + e_3)(e_2/2)^3 \exp(-500/T);$$

$$r_a = kny_1; \quad r_c = kny_2; \quad r_2 = k_2 n; \quad r_3 = k_3 n;$$

$$k_2 = \sum_{i=1}^{3} y_i k_{2i}; \quad k_3 = \sum_{i=1}^{3} y_i k_{3i}; \tag{3.9}$$

$$n = 273 \frac{p[\text{bar}]}{T_0[\text{K}]};$$

$$e_{2T} = \frac{2}{\exp(960/T) - 1}$$

where $W(t)$ is the discharge power density measured in kW/cm^3, p_e is measured in μs^{-1}, and the constants k are calculated using the following expressions [2, 27]:

$$k = 240/T^{1/2};$$

$$k_{31} = A(t) \exp(4.138 + 7.945x - 631.24x^2 + 2239x^3);$$

$$k_{32} = A(t) \exp(-1.863 + 213.3x - 2796.2x^2 + 9001.9x^3);$$

$$k_{33} = A(t) \exp(-3.276 + 291.4x - 3831.8x^2 + 12688x^3); \tag{3.10}$$

$$k_{21} = 1.16 \times 10^3 \exp(-59.3x);$$

$$k_{22} = 8.55 \times 10^2 \exp(-69x);$$

$$k_{23} = 1.3 \times 10^3 \exp(-40.6x)$$

where $x = T^{-1/3}$, $A(t) = (T/273)(1 + e_{2T}/2)^{-3}$, and temperature T is expressed in K.

Finally, the dynamics of the gas temperature is described by the following equation:

$$\frac{dT}{dt} = \frac{y_1}{C_V} (500r_3 f_3 + 960r_2(e_2 - e_{2T})) + 2.7 \frac{W(t)q_T}{nC_V}, \tag{3.11}$$

where $C_V = 2.5(y_1 + y_2) + 1.5y_3$.

3.1.3 Optical pumping

Initial support for optical pumping is included in the co2amp code. We assume instant excitation (pump pulse is short compared to vibrational relaxation). The fraction of CO_2 molecules excited by the optical pulse is calculated as

$$\frac{N^*}{N} = \frac{1 - \exp(-\Phi\sigma)}{2} \tag{3.12}$$

where N and $N*$ are the total density of the CO_2 molecules and the density of the excited molecules respectively, Φ is the flux of the pumping photons, and σ is the absorption cross-section.

An adjustment then is made to the average number of quanta in the asymmetric stretch vibration:

$$e_3 = e_3' + \frac{N^*}{N} \tag{3.13}$$

where $e_3' = \frac{1}{\exp\left(\frac{3350}{T_0}\right)-1}$ is the value of e_3 before excitation, and T_0 is the initial temperature of the gas.

For optical pumping at $\sim 3\ \mu$m through a combinational vibration $(10^01, 02^01)$, e_2 also increases as follows:

$$e_2 = e_2' + 2\frac{N^*}{N} \times \frac{e_2'}{2e_1' + e_2'} \tag{3.14}$$

where $e_1' = \frac{1}{\exp\left(\frac{1920}{T_2}\right)-1}$, $e_2' = \frac{2}{\exp\left(\frac{960}{T_2}\right)-1}$, and the last term takes into account the equilibrium energy distribution between the coupled symmetric stretch and bending vibrations. Several iterations are needed to accurately determine e_2: The first iteration is done for $T_2 = T_0$; a corrected value of T_2 is then calculated using the first of the equations (3.7), and is used in the next iteration for calculating e_2, and so forth.

For optical pumping, the dynamics of vibrational relaxation is modeled using equations (3.8) with $p_{e2} = p_{e3} = p_{e4} = 0$.

3.2 Amplification

3.2.1 Laser transitions

Fig. 3.1 shows the vibrational levels and laser transitions included in the `co2amp` amplification model (because of the lack of the spectroscopic data, the sequence and hot bands currently are only supported for natural isotopologue of CO_2 $(626$[1]$)$.

3.2.2 Main equations

Amplification is simulated in the fast time-frame moving with the pulse using the following equations that also take into account rotational relaxation [8, 28]:

$$\begin{aligned}
\frac{\partial E}{\partial z} &= -\sum_J \rho_J, \\
\frac{\partial \rho_J}{\partial t} + \left(2\pi i(\nu_c - \nu_{0J}) + \frac{1}{\tau_2}\right)\rho_J &= -\frac{\sigma_J n_J E}{2\tau_2}, \\
\frac{\partial n_J}{\partial t} + \frac{n_J - n_J^0}{\tau_R} &= 4(\rho_J E^* + c.c.),
\end{aligned} \tag{3.15}$$

where summation is done over all rotational-vibrational transitions of all CO_2 isotopologues, and

E - complex field envelope,

ρ_J - polarization of the medium,

z - linear coordinate along the direction of beam propagation,

t - time,

n_J - population inversion of the transition (difference of population densities of upper and lower levels),

n_J^0 - equilibrium population inversion of the transition,

ν_c - carrier frequency,

ν_{0J} - transition frequency in the line center,

σ_J - transition cross-section in the line center,

τ_2 - polarization dephasing time,

---

[1]A 3-digit notation commonly is used for designating the isotopologues (molecules with different isotopic composition) of carbon dioxide. In this notation *2*, *3* and *4* correspondingly stand for ^{12}C, ^{13}C and ^{14}C; *6*, *7* and *8* represent correspondingly ^{16}O, ^{17}O and ^{18}O. *626* denotes a CO_2 molecule with natural isotopic composition: ^{16}O-^{12}C-^{16}O.
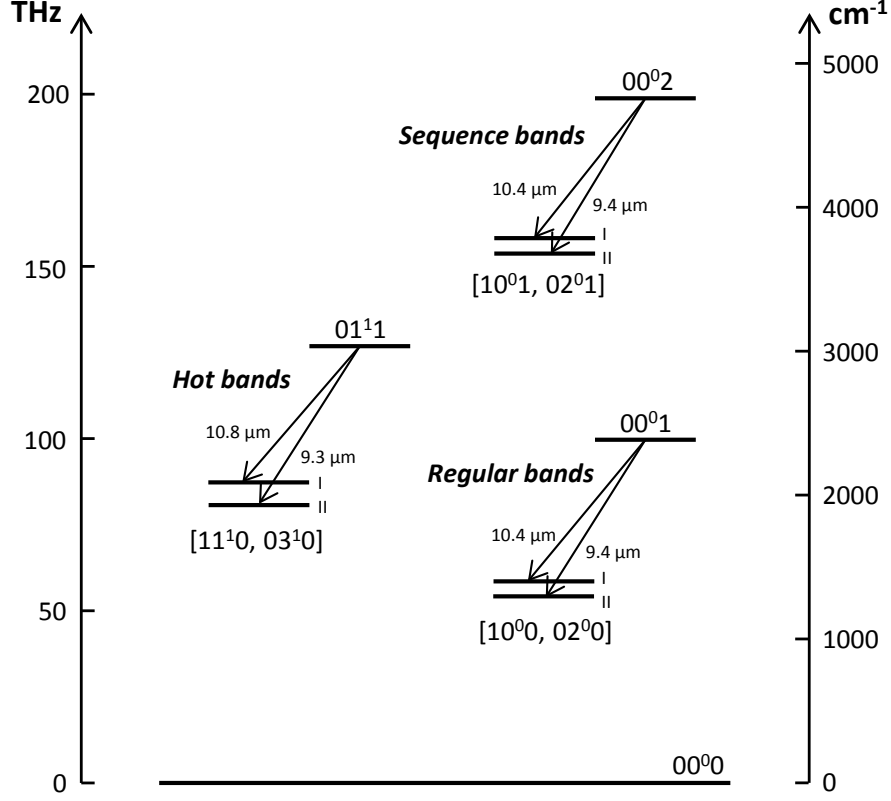
Figure 3.1: Vibrational transitions included in the amplification model. Wavelengths are given for natural CO_2 isotopologue (*626*).

τ_R - rotational relaxation time.

Transition frequencies of P and R transitions are calculated as follows:

$$\nu_J = \begin{cases} V + B_U(J-1)J - B_L J(J+1) & (P) \\ V + B_U(J+1)(J+2) - B_L J(J+1) & (R) \end{cases} \tag{3.16}$$

where J is the rotational quantum number, V is the vibrational constant of the corresponding transition, and, B_U and B_L the rotational constants of the upper and lower level of the transition correspondingly. The numerical values of the molecular constants used in the program are listed in Appendix B.

The transition cross-section in the line center is calculated [13]

$$\sigma_J[\text{m}^2] = \frac{(\lambda_J[\text{m}])^2 A_J[\text{s}^{-1}]}{4} \times \frac{\tau_2[\text{s}]}{\pi} \tag{3.17}$$

where the first term defines the integral cross-section of the rotational line, and the second term is the maximum of the normalized Lorentzian profile of a line with width $2\pi\Delta\nu_{HWHM} = 1/\tau_2$.

Population inversion in the rotational equilibrium is calculated as

$$n_J^0 = \begin{cases} z(J-1)N_U - z(J)N_L & (P) \\ z(J+1)N_U - z(J)N_L & (R) \end{cases} \tag{3.18}$$

where N_U and N_L are the population densities of the corresponding upper and lower *vibrational* levels, and

$z(J)$ is the Boltzmann distribution:

$$z(J) = \begin{cases} 2\dfrac{hB}{kT}(2J+1)\exp\left(-\dfrac{hB}{kT}J(J+1)\right) & (626, 636, 828, 838) \\[2ex] \dfrac{hB}{kT}(2J+1)\exp\left(-\dfrac{hB}{kT}J(J+1)\right) & (628, 638) \end{cases} \tag{3.19}$$

where $h = 6.62606957 \times 10^{-34}$ J·s and $k = 1.3806488 \times 10^{-23}$ J/K

Optical intensity I is related to the field amplitude as follows:

$$I[\text{W/m}^2] = 2h[\text{J·s}]\nu_c[\text{s}^{-1}]|E|^2 \tag{3.20}$$

Dephasing and relaxation times are defined by the following equations:

$$\tau_2[\text{s}] = \frac{10^{-6}}{\pi \times 7.61 \times 750 \times (P_{CO2} + 0.733P_{N2} + 0.64P_{He})}$$
$$\tau_R[\text{s}] = \frac{10^{-7}}{750 \times (1.3P_{CO2} + 1.2P_{N2} + 0.6P_{He})} \tag{3.21}$$

where pressure P is measured in bars.

3.2.3 Populations

In the approximation used in the `co2amp` model, the processes of pumping and vibrational relaxation are slow compared to the duration of the pulse. Thus, during the pulse only the stimulated transitions contribute to the change of the populations of the vibrational levels.

In the fast time-frame associated with the pulse there is no equilibrium in the vibrational energy distribution, and a proper population dynamics rather than the temperature model must be used. Thus, during the amplification, population of each rotational-vibrational level is considered independently. After the pulse leaves the active medium, the energy distribution within each vibrational mode becomes normalized quickly, and can be described by the temperature model again.

An important simplification used in the model is the assumption that vibrational temperatures T_2 and T_3 are the same for all CO_2 isotopologues. This assumption can be justified by the relatively small energy mismatch between vibrational levels of different isotopic species of the same molecule, and thus, fast intermolecular V-V energy exchange. However, this assumption may not hold if the time-delay between two consecutive passes of a pulse through the amplifier is short compared to the relaxation times of intra-mode and inter-isotopic vibrational energy.

Initial populations of vibrational levels are calculated for each isotopologue and for each band using the

15

following equations:

Regular band

$$N_{00^01} = \frac{N}{\mathcal{Q}} \exp\left(\frac{-3380}{T_3}\right)$$

$$N_{[10^00,02^00]_I} = N_{[10^00,02^00]_{II}} = \frac{N}{\mathcal{Q}} \exp\left(\frac{-2 \times 960}{T_2}\right)$$

Sequence band

$$N_{00^02} = \frac{N}{\mathcal{Q}} \exp\left(\frac{-2 \times 3380}{T_3}\right)$$

$$N_{[10^01,02^01]_I} = N_{[10^01,02^01]_{II}} = \frac{N}{\mathcal{Q}} \exp\left(\frac{-2 \times 960}{T_2}\right) \exp\left(\frac{-3380}{T_3}\right)$$

$$\text{(3.22)}$$

Hot band

$$N_{01^11} = \frac{N}{\mathcal{Q}} \exp\left(\frac{-3380}{T_3}\right) \exp\left(\frac{-960}{T_2}\right)$$

$$N_{[11^10,03^10]_I} = N_{[11^10,03^10]_{II}} = \frac{N}{\mathcal{Q}} \exp\left(\frac{-3 \times 960}{T_2}\right)$$

where N is the density of CO_2 molecules, and $\mathcal{Q}$ the partition function [29]:

$$\frac{1}{\mathcal{Q}} = \left(1 - \exp\left(\frac{-1920}{T_2}\right)\right) \times \left(1 - \exp\left(\frac{-3380}{T_3}\right)\right) \times \left(1 - \exp\left(\frac{-960}{T_2}\right)\right)^2 \qquad \text{(3.23)}$$

Change of the populations in the regular band due to stimulated transitions is calculated for each vibrational level using the last of the equations 3.15:

$$\frac{d}{dt} N_{00^01} = 2 \sum_{J(00^01 \to [10^00,02^00]_{I,II})} (\rho_J E^* + c.c.)$$

$$\frac{d}{dt} N_{[10^00,02^00]_I} = -2 \sum_{J(00^01 \to [10^00,02^00]_I)} (\rho_J E^* + c.c.) \qquad \text{(3.24)}$$

$$\frac{d}{dt} N_{[10^00,02^00]_{II}} = -2 \sum_{J(00^01 \to [10^00,02^00]_{II})} (\rho_J E^* + c.c.)$$

where summation is done over all rotational transitions originating or ending at the corresponding vibrational level. Analogous equations are used for the sequence and the hot bands.

Changes of the average quantum numbers in the vibrational modes due to stimulated transitions are calculated as follows:

$$\Delta e_3 = \frac{\Delta N_U}{N},$$

$$\Delta e_2 = -2 \frac{\Delta N_U}{N} \times \frac{e_2'}{2e_1' + e_2'} \qquad \text{(3.25)}$$

wherein the last term in the second equation takes into account the equilibrium energy distribution between the coupled symmetric stretch and bending vibrations, $e_1' = \frac{1}{\exp\left(\frac{1920}{T_2}\right)-1}$, $e_2' = \frac{2}{\exp\left(\frac{960}{T_2}\right)-1}$, and T_2 is the vibrational temperature before the propagation of the pulse.

New vibrational temperatures then are calculated using the first and second equations 3.7.

3.3 Propagation

Beam propagation between layout elements is calculated using Huygens-Fresnel integration at each time-step of the pulse time-frame. In the general case, the field in a given position (x', y') of the output plane is calculated by integrating the contributions from each point (x, y) of the input plane, taking into account the phase delay:

$$E(x', y') = \int_x \int_y E(x, y) \frac{e^{i\kappa R}}{i\lambda R} dx dy \tag{3.26}$$

where κ is the wave number, λ is the wavelength, and $R = \sqrt{(x - x')^2 + (y - y')^2 + \Delta z^2}$ is the distance between points (x, y) and (x', y'); Δz is the distance between the centers of the input and the output planes.

In the case of radially symmetric beam used in our model, calculations can be considerably accelerated by taken into account that the field is the same in all points at equal distance from the beam axis. In this case integration can be done by summing the contributions of concentric rings in the input plane as shown in the Fig. 3.2.
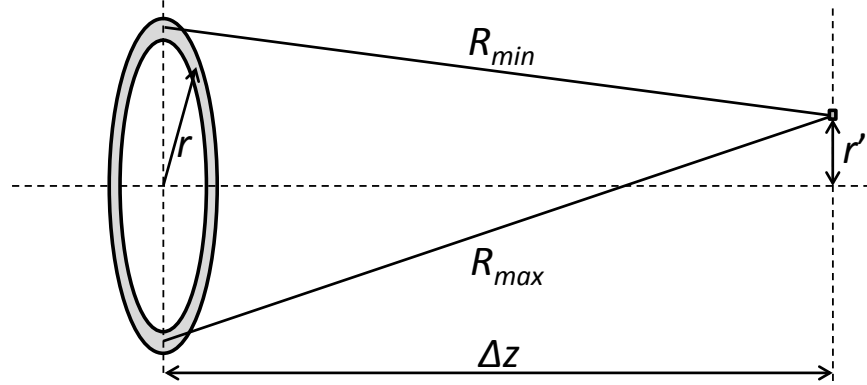
Figure 3.2: Huygens-Fresnel integration in the axial-symmetric system: Contribution of a field from a concentric ring in the input plane to a field in a point in the output plane.

The field in a given point with radial coordinate r' in the output plane is then calculated as

$$E(r') = \int_r E(r) \frac{e^{-i\kappa R}}{i\lambda R} J_0(\kappa \Delta R/2) dS \tag{3.27}$$

where $dS = \pi(r + dr/2)^2 - \pi(r - dr/2)^2$ is the area of the ring, $R = (R_{max} + R_{min})/2$, $\Delta R = R_{max} - R_{min}$, $R_{max} = \sqrt{(r + r')^2 + \Delta z^2}$, $R_{min} = \sqrt{(r - r')^2 + \Delta z^2}$, and J_0 is the Bessel function.

3.4 Optical elements

Optical elements change the electric field as described by the following formulas. In them, $E(t, r)$ is the field in the input of the element, and $E'(t, r)$ - after passing through the element.

PROBE

(*Passive surface*)

$$E'(t, r) = E(t, r) \tag{3.28}$$

MASK

(*Opaque circular screen*)

$$E'(t,r) = \begin{cases} 0 & r < \mathcal{R} \\ E(t,r) & r \geq \mathcal{R} \end{cases} \tag{3.29}$$

where $\mathcal{R}$ is the radius of the screen.

ATTENUATOR

(*Ideal neutral density filter. Can be used as an ideal amplifier by setting $\mathcal{T} > 1$.*)

$$E'(t,r) = E(t,r)\sqrt{\mathcal{T}} \tag{3.30}$$

where $\mathcal{T}$ is transmittance.

LENS

(*Ideal lens without aberrations*)

$$E'(t,r) = E(t,r)\exp\left(\pi i \frac{r^2}{\lambda_c F}\right) \tag{3.31}$$

where F is the focal length of the lens, and λ_c is the central wavelength.

WINDOW, AIR

(*Flat transparent window with zero reflection and absorption losses, or air*)

Note: A normal incidence is assumed. In the case of an oblique incidence, the user should take appropriate measures for accounting for the reduced optical intensity on the surface, and the increased propagation length (effective thickness). However, if '-Brewster' modifier is used in the material's name (KCl-Brewster, Si-Brewster, etc.), the necessary adjustments are performed automatically for the Brewster's angle calculated at the central wavelength.

Linear dispersion

$$\begin{aligned} \widehat{E}(\nu,r) &= \mathcal{F}(E(t,r)) \\ \widehat{E}'(\nu,r) &= \widehat{E}(\nu,r)\exp\left(-2\pi i\nu\frac{\Theta}{c}\left(n_0(\nu) - n_0(\nu_c) - \nu_c\frac{dn_0}{d\nu}\right)\right) \\ E'(t,r) &= \mathcal{F}^{-1}(\widehat{E}'(\nu,r)) \end{aligned} \tag{3.32}$$

where $\widehat{E}(\nu,r)$ is the field in the frequency domain, $\mathcal{F}$ and $\mathcal{F}^{-1}$ are the Fourier-transform and inverse-Fourier-transform functions, ν is the frequency, ν_c is the central frequency, n_0 is the linear component of the index of refraction, and Θ is the thickness of the window. The dispersion formulas used for calculating n_0 are given in Appendix C.

Nonlinear interaction

$$E'(t,r) = E(t,r)\exp\left(-2\pi i\nu_c\frac{\Theta}{c}n_2 I(t,r)\right) \tag{3.33}$$

where n_2 is the nonlinear refractive index, and $I(t,r)$ is the field intensity. The numerical values of n_2 used in the program are given in Appendix C.

STRETCHER

(*Stretcher or compressor*)

$$
\begin{aligned}
\widehat{E}(\nu, r) &= \mathcal{F}(E(t, r)) \\
\widehat{E}'(\nu, r) &= \widehat{E}(\nu, r) \exp\left(-\pi i(\nu - \nu_c)^2 \mathcal{S}\right) \\
E'(t, r) &= \mathcal{F}^{-1}(\widehat{E}'(\nu, r))
\end{aligned}
\tag{3.34}
$$

where $\mathcal{S}$ is the stretching factor (in s/Hz, positive for the red chirp).

BANDPASS

(*Band-pass filter*)

$$
\begin{aligned}
\widehat{E}(\nu, r) &= \mathcal{F}(E(t, r)) \\
\widehat{E}'(\nu, r) &= \begin{cases} 0 & \nu < (\nu_b - \Delta\nu/2); \ \nu > (\nu_b + \Delta\nu/2) \\ \widehat{E}(\nu, r) & (\nu_b - \Delta\nu/2) \leq \nu \leq (\nu_b + \Delta\nu/2) \end{cases} \\
E'(t, r) &= \mathcal{F}^{-1}(\widehat{E}'(\nu, r))
\end{aligned}
\tag{3.35}
$$

where ν_b is the band center, and $\Delta\nu$ the bandwidth of the filter.

APODIZER

(*Apodizing filter*)

$$
E'(t, r) = \begin{cases} E(r, t) & r \leq (1 - \alpha)\mathcal{R} \\ E(r, t)\sqrt{sin^2\left(\frac{\mathcal{R}-r}{2\alpha\mathcal{R}}\pi\right)} & r > (1 - \alpha)\mathcal{R} \end{cases}
\tag{3.36}
$$

where $\mathcal{R}$ is the maximum radius of the filter ("field"), and α is a constant ($0 \leq \alpha \leq 1$).

Appendices

Appendix A

Cross-sections of excitation processes

Effective cross-sections are expressed in Å; their numerical values in the nodes are given in the tables below (linear interpolation must be used for determining the values in intermediate points); the data and citations are reproduced from [15].

The following notation for cross-sections is used:

Q_{m1} - Transport cross-section of CO_2 [17];

Q_{m2} - Transport cross-section of N_2 [10];

Q_{m3} - Transport cross-section of He [17];

Q - Cross-section of resonant excitation of N_2 rotation [21, 4];

Q_{11} - Cross-section of the process $(000) \rightarrow (01^10)$ [17];

Q_{12} - Cross-section of the process $(000) \rightarrow (100 + 020)$ [17];

$Q_{13}...Q_{16}$ - Cross-sections of resonant processes around 3.8 eV [17];

Q_{17} - Cross-section of the process $(000) \rightarrow (001)$ [17];

$Q_{18}...Q_{1,10}$ - Cross-sections of electronic excitation and ionization of CO_2 [12];

$Q_{21}...Q_{28}$ - Cross-sections of the process $N_2(v = 0) \rightarrow N_2(v = 1...8)$ [22, 23, 7];

$Q_{29}...Q_{2,15}$ - Cross-sections of electronic excitation and ionization of N_2 [7].

Table A.1: Cross-sections and energies for discharge pumping

u_i	Q_{m1}	u_i	Q_{m2}	u_i	Q_{m3}	u_i	Q
0	140	0	1.4	0	5	0.0015	0
0.04	84	0.001	1.4	0.01	5.4	0.05	0.1
0.1	55	0.002	1.6	0.1	5.8	0.25	0.65
0.3	21	0.008	2	0.2	6.2	0.5	1.15
0.5	10.8	0.01	2.2	1	6.5	0.8	2
0.6	9.4	0.04	4	2	6.1	1	2.65
1	5.7	0.08	6	7	5	1.5	5.6
1.7	5	0.1	6.5	10	4.1	1.8	7.5
2	5.1	0.2	8.8	20	3	1.9	8.2
2.5	6	0.3	9.8			2	8.6
3	7.7	0.4	10			2.15	8.95
4.1	9.4	1	10			2.43	9
5	14.5	1.2	11			2.6	8.9
7.4	10	1.4	12.5			2.75	8.4
10	11.7	1.8	20			2.9	7.65
20	16	2	25			3.25	6.2
27	16.3	2.5	30			3.6	5.1
50	13	3	26			4	4.5
		4	15			4.5	4.16
		5	12			5	3.97
		7	10			5.5	3.93
		10	10			7	4.17
		14	11			9	4.46
		18	12.2			11	4.42
		20	12			15	3.94
		30	10			22	3.15
		100	10			25	3.05

Table A.2: Cross-sections and energies for discharge pumping - continued

u_i	Q_{11}	u_i	Q_{12}	u_i	Q_{13}	u_i	Q_{14}	u_i	Q_{15}
0.083	0	0.167	0	0.252	0	2.37	0	2.37	0
0.085	0.36	0.2	0.54	2.7	0.25	3	0.26	3	0.17
0.09	1.04	0.25	0.82	3	0.4	3.5	0.52	3.65	0.33
0.1	1.6	0.3	0.82	3.3	0.6	4	0.5	3.8	0.31
0.12	1.84	0.5	0.68	3.6	0.65	4.5	0.22	4	0.21
0.14	2.12	0.7	0.56	4.5	0.23	4.6	0.1	4.3	0.1
0.16	2.16	1	0.47	4.6	0.1	5	0	5	0
0.2	2.08	1.4	0.45	5	0				
0.3	1.76	2	0.55						
0.4	1.52	3	1.15						
0.5	1.28	3.9	1.83						
0.6	1.08	4.5	1.4						
0.8	0.8	5	0.4						
1	0.58	6	0.28						
1.2	0.48	10	0.2						
1.6	0.34	20	0.1						
1.8	0.35								
2	0.4								
2.5	0.64								
3	1.04								
3.7	1.4								
4	1.36								
4.2	1.2								
4.5	0.92								
5	0.53								
6	0.4								
8	0.36								
9	0.28								
10	0.16								
10.1	0								
$u_{11} = 0.083$ eV		$u_{12} = 0.167$ eV		$u_{13} = 0.252$ eV		$u_{14} = 0.339$ eV		$u_{15} = 0.422$ eV	

u_i	Q_{16}	u_i	Q_{17}	u_i	Q_{18}	u_i	Q_{19}	u_i	$Q_{1,10}$
2.5	0	0.29	0	7	0	10.5	0	13.8	0
3	0.19	0.3	0.44	8	0.5	11.5	0.56	15	0.1
3.6	0.245	0.35	0.65	8.4	0.6	14	0.8	16	0.13
4	0.21	0.4	0.73	9	0.46	20	1.2	17	0.17
5.07	0	0.5	0.84	10	0.175	30	2	30	1.55
		0.8	1	10.5	0	50	4	40	2.1
		1	1						
		2	0.78						
		6	0.37						
		10	0.25						
		50	0						
$u_{16} = 2.5$ eV		$u_{17} = 0.29$ eV		$u_{18} = 7$ eV		$u_{19} = 10.5$ eV		$u_{1,10} = 13.8$ eV	

Table A.3: Cross-sections and energies for discharge pumping - continued

u_i	Q_{21}	u_i	Q_{22}	u_i	Q_{23}	u_i	Q_{24}	u_i	Q_{25}
0.29	0	1.83	0	1.9	0	2.05	0	2.1	0
0.5	0.0052	1.9	0.208	2	0.416	2.1	0.416	2.15	0.208
0.8	0.0083	2	1.46	2.1	1.33	2.2	1.16	2.2	0.541
1	0.0104	2.05	2.29	2.2	1.87	2.26	1.58	2.3	0.915
1.2	0.0166	2.1	1.66	2.3	1.25	2.55	0	2.46	1.12
1.3	0.0728	2.2	0.79	2.36	0.208	2.75	0.832	2.5	1.12
1.4	0.135	2.35	0.208	2.42	0	2.77	0	2.6	0.208
1.6	0.25	2.45	1.98	2.5	0.499	3	0.208	2.62	0
1.8	0.52	2.5	1.78	2.61	0.915	3.05	0.208	2.68	0
1.9	0.832	2.62	0.208	2.7	0.624	3.25	0	2.8	0.416
2	3.02	2.75	1.04	2.75	0.208			2.9	0.75
2.05	3.12	2.95	1.66	2.8	0			3	0
2.1	2.08	3.05	0.624	2.92	0.416			3.2	0.25
2.15	1.25	3.2	0.208	3	0.208			3.3	0.125
2.2	0.832	3.4	0.208	3.25	0.208			3.35	0
2.3	2.9	4	0	3.31	0				
2.45	1.04								
2.53	1.25								
2.6	1.75								
2.62	2.08								
2.68	1.73								
2.73	0.416								
2.85	0.32								
2.92	0.416								
3.12	0.728								
3.3	0.52								
4	0								
$u_{21} = 0.29$ eV		$u_{22} = 0.58$ eV		$u_{23} = 0.87$ eV		$u_{24} = 1.16$ eV		$u_{25} = 1.45$ eV	

u_i	Q_{26}	u_i	Q_{27}	u_i	Q_{28}	u_i	Q_{29}	u_i	$Q_{2,10}$
2.3	0	2.4	0	2.6	0	5	0	6.8	0
2.4	0.75	2.5	0.208	2.7	0.208	5.9	0.41	7.1	0.57
2.5	1.04	2.75	0.75	2.9	0.29	6.1	0.41	8.1	0.57
2.55	1.12	3	0	3	0.208	7	0.07	8.6	0.25
2.6	1.04	3.2	0.166	3.1	0	9	0	9.5	0.12
2.65	0.624	3.3	0.146	3.2	0			20.7	0
2.7	0.416	3.4	0	3.3	1.04				
2.8	0.208			3.4	0				
2.9	0.125								
3	2.5								
3.1	0.166								
3.2	0								
$u_{26} = 1.74$ eV		$u_{27} = 2.03$ eV		$u_{28} = 2.32$ eV		$u_{29} = 5$ eV		$u_{2,10} = 6.8$ eV	

u_i	$Q_{2,11}$	u_i	$Q_{2,12}$	u_i	$Q_{2,13}$	u_i	$Q_{2,14}$	u_i	$Q_{2,15}$
8.4	0	11.25	0	12.5	0	14	0	15.6	0
8.7	0.42	13.8	0.41	13	0.4	14.3	1.7	18	0.1
9.1	0.42	14	1	13.6	0.4	14.8	1.7	20	0.21
10	0.3	14.7	1	14	0.16	15.6	0.2	50	2.52
20.7	0	15	0.25	20.7	0	20.6	0.2	100	2.52
		65	0			25.4	2.8		
						100	2.8		
$u_{2,11} = 8.4$ eV		$u_{2,12} = 11.25$ eV		$u_{2,13} = 12.5$ eV		$u_{2,14} = 14$ eV		$u_{2,15} = 15.6$ eV	

Appendix B

Molecular constants

The vibrational and rotational constants V and B are listed in Table B.1.

Einstein coefficients A of the laser transitions included in the simulations are summarized in Tables B.2-B.7. Except for the 10-micron transitions of *838* isotopologue, data are taken from the HITRAN2016 database [11] (Einstein coefficients) and our fit of HITRAN data with equation (3.16) (V and B).

For 10-micron transitions of *838* (not included in the HITRAN datavase), V and B constants are taken from [18]; Einstein coefficients are assumed to be the same as for the corresponding 9-micron transitions (according to Freed's gain measurements [9]).

Table B.1: Molecular constants of CO_2 isotopologues, Hz

	626	628	828	636	638	838
$00^01 \rightarrow [10^00, 02^00]_{I,II}$ ('Regular band')						
$V(00^01 - I)$	2.8809e13	2.8969e13	2.8988e13	2.7384e13	2.7692e13	2.7839e13
$V(00^01 - II)$	3.1889e13	3.2158e13	3.2489e13	3.0508e13	3.061e130	3.0786e13
$B(00^01)$	1.1589e10	1.0936e10	1.0303e10	1.1593e10	1.0939e10	1.0315e10
$B([10^00, 02^00]_I)$	1.1683e10	1.1034e10	1.0403e10	1.1668e10	1.1019e10	1.0403e10
$B([10^00, 02^00]_{II})$	1.1687e10	1.1019e10	1.0375e10	1.1700e10	1.1031e10	1.0394e10
$00^02 \rightarrow [10^01, 02^01]_{I,II}$ ('Sequence band')						
$V(00^02 - I)$	2.8737e13	2.8911e13	-	2.7300e13	-	-
$V(00^02 - II)$	3.1792e13	3.2029e13	-	3.0453e13	-	-
$B(00^02)$	1.1497e10	1.0859e10	-	1.1512e10	-	-
$B([10^01, 02^01]_I)$	1.1588e10	1.0955e10	-	1.1585e10	-	-
$B([10^01, 02^01]_{II})$	1.1598e10	1.0946e10	-	1.1623e10	-	-
$01^1e1 \rightarrow [11^1e0, 03^1e0]_{I,II}$ ('Hot-e band')						
$V(01^1e1 - I)$	2.7796e13	2.7964e13	2.0190e13	2.6476e13	2.6749e13	-
$V(01^1e1 - II)$	3.2124e13	3.2388e13	3.2690e13	3.0689e13	3.0832e13	-
$B(01^1e1)$	1.1602e10	1.0949e10	1.0324e10	1.1605e10	1.0953e10	-
$B([11^1e0, 03^1e0]_I)$	1.1687e10	1.1036e10	1.0412e10	1.1676e10	1.1028e10	-
$B([11^1e0, 03^1e0]_{II})$	1.1695e10	1.1032e10	1.0398e10	1.1702e10	1.1040e10	-
$01^1f1 \rightarrow [11^1f0, 03^1f0]_{I,II}$ ('Hot-f band')						
$V(01^1f1 - I)$	2.7796e13	2.7964e13	2.8019e13	2.6476e13	2.6749e13	-
$V(01^1f1 - II)$	3.2124e13	3.2388e13	3.2690e13	3.0689e13	3.0832e13	-
$B(01^1f1)$	1.1620e10	1.0965e10	1.0338e10	1.1623e10	1.0970e10	-
$B([11^1f0, 03^1f0]_I)$	1.1716e10	1.1063e10	1.0437e10	1.1703e10	1.1053e10	-
$B([11^1f0, 03^1f0]_{II})$	1.1723e10	1.1055e10	1.0417e10	1.1733e10	1.1066e10	-

Table B.2: Einstein coefficients A of laser transitions of '626' CO_2, s^{-1}

J	Regular				Sequence				Hot-e				Hot-f			
	10P	10R	9P	9R	10P	10R	9P	9R	10P	10R	9P	9R	10P	10R	9P	9R
0	-	-	-	-	-	-	-	-	-	-	-	-	-	-	-	-
1	-	0.130	-	0.145	-	0.324	-	0.322	-	0.106	-	0.130	-	0.135	-	0.166
2	0.260	-	0.289	-	0.809	-	0.800	-	-	-	-	-	0.176	-	0.216	-
3	-	0.168	-	0.187	-	0.361	-	0.359	-	0.147	-	0.182	-	0.155	-	0.191
4	0.222	-	0.247	-	0.484	-	0.478	-	0.188	-	0.230	-	0.188	-	0.231	-
5	-	0.178	-	0.199	-	0.376	-	0.374	-	0.159	-	0.197	-	0.162	-	0.201
6	0.212	-	0.235	-	0.447	-	0.442	-	0.188	-	0.229	-	0.186	-	0.227	-
7	-	0.184	-	0.205	-	0.384	-	0.383	-	0.164	-	0.204	-	0.166	-	0.206
8	0.206	-	0.229	-	0.432	-	0.427	-	0.185	-	0.226	-	0.184	-	0.225	-
9	-	0.186	-	0.209	-	0.389	-	0.389	-	0.167	-	0.208	-	0.169	-	0.210
10	0.203	-	0.225	-	0.423	-	0.418	-	0.183	-	0.223	-	0.182	-	0.222	-
11	-	0.188	-	0.212	-	0.392	-	0.394	-	0.169	-	0.212	-	0.170	-	0.212
12	0.200	-	0.223	-	0.417	-	0.413	-	0.182	-	0.221	-	0.180	-	0.220	-
13	-	0.190	-	0.215	-	0.395	-	0.398	-	0.170	-	0.214	-	0.172	-	0.215
14	0.198	-	0.221	-	0.412	-	0.409	-	0.180	-	0.219	-	0.179	-	0.219	-
15	-	0.191	-	0.217	-	0.396	-	0.401	-	0.171	-	0.216	-	0.172	-	0.217
16	0.196	-	0.219	-	0.408	-	0.406	-	0.179	-	0.217	-	0.177	-	0.217	-
17	-	0.192	-	0.218	-	0.398	-	0.405	-	0.171	-	0.218	-	0.173	-	0.218
18	0.195	-	0.218	-	0.405	-	0.403	-	0.178	-	0.216	-	0.176	-	0.216	-
19	-	0.192	-	0.220	-	0.399	-	0.408	-	0.172	-	0.220	-	0.173	-	0.220
20	0.193	-	0.217	-	0.402	-	0.401	-	0.177	-	0.215	-	0.175	-	0.215	-
21	-	0.192	-	0.222	-	0.399	-	0.411	-	0.172	-	0.221	-	0.174	-	0.222
22	0.192	-	0.216	-	0.399	-	0.400	-	0.176	-	0.214	-	0.174	-	0.214	-
23	-	0.193	-	0.223	-	0.400	-	0.414	-	0.172	-	0.223	-	0.174	-	0.223
24	0.190	-	0.215	-	0.396	-	0.398	-	0.175	-	0.213	-	0.173	-	0.214	-
25	-	0.193	-	0.225	-	0.400	-	0.417	-	0.172	-	0.224	-	0.174	-	0.224
26	0.189	-	0.215	-	0.393	-	0.397	-	0.175	-	0.212	-	0.171	-	0.213	-
27	-	0.193	-	0.226	-	0.400	-	0.420	-	0.172	-	0.226	-	0.174	-	0.226
28	0.188	-	0.214	-	0.390	-	0.396	-	0.174	-	0.211	-	0.170	-	0.212	-
29	-	0.193	-	0.228	-	0.400	-	0.423	-	0.172	-	0.227	-	0.174	-	0.227
30	0.186	-	0.214	-	0.387	-	0.395	-	0.173	-	0.210	-	0.169	-	0.212	-
31	-	0.192	-	0.229	-	0.399	-	0.425	-	0.171	-	0.229	-	0.174	-	0.229
32	0.185	-	0.213	-	0.384	-	0.394	-	0.172	-	0.209	-	0.168	-	0.211	-
33	-	0.192	-	0.231	-	0.399	-	0.428	-	0.171	-	0.230	-	0.173	-	0.230
34	0.183	-	0.213	-	0.381	-	0.393	-	0.171	-	0.208	-	0.167	-	0.211	-
35	-	0.192	-	0.232	-	0.398	-	0.432	-	0.171	-	0.231	-	0.173	-	0.231
36	0.182	-	0.212	-	0.378	-	0.393	-	0.170	-	0.208	-	0.166	-	0.210	-
37	-	0.191	-	0.234	-	0.397	-	0.435	-	0.170	-	0.233	-	0.173	-	0.233
38	0.181	-	0.212	-	0.375	-	0.392	-	0.169	-	0.207	-	0.164	-	0.210	-
39	-	0.191	-	0.236	-	0.396	-	0.438	-	0.170	-	0.234	-	0.172	-	0.234
40	0.179	-	0.212	-	0.372	-	0.392	-	0.168	-	0.207	-	0.163	-	0.209	-
41	-	0.190	-	0.237	-	0.395	-	0.441	-	0.169	-	0.236	-	0.172	-	0.236
42	0.177	-	0.212	-	0.369	-	0.392	-	0.167	-	0.206	-	0.162	-	0.209	-
43	-	0.190	-	0.239	-	0.393	-	0.444	-	0.168	-	0.237	-	0.171	-	0.237
44	0.176	-	0.211	-	0.366	-	0.392	-	0.166	-	0.205	-	0.161	-	0.209	-
45	-	0.189	-	0.241	-	0.392	-	0.447	-	0.168	-	0.239	-	0.171	-	0.239
46	0.174	-	0.211	-	0.363	-	0.391	-	0.165	-	0.205	-	0.159	-	0.208	-
47	-	0.188	-	0.242	-	0.390	-	0.451	-	0.167	-	0.240	-	0.170	-	0.240
48	0.173	-	0.211	-	0.359	-	0.391	-	0.164	-	0.204	-	0.158	-	0.208	-
49	-	0.187	-	0.244	-	0.388	-	0.454	-	0.166	-	0.241	-	0.169	-	0.242
50	0.171	-	0.211	-	0.356	-	0.391	-	0.163	-	0.204	-	0.157	-	0.208	-
51	-	0.186	-	0.246	-	0.387	-	0.458	-	0.165	-	0.243	-	0.168	-	0.243
52	0.169	-	0.211	-	0.352	-	0.391	-	0.162	-	0.203	-	0.155	-	0.207	-
53	-	0.185	-	0.248	-	0.385	-	0.461	-	0.164	-	0.244	-	0.167	-	0.245
54	0.167	-	0.211	-	0.349	-	0.391	-	0.161	-	0.203	-	0.154	-	0.207	-
55	-	0.184	-	0.249	-	0.382	-	0.465	-	0.163	-	0.246	-	0.167	-	0.246
56	0.166	-	0.211	-	0.345	-	0.391	-	0.160	-	0.202	-	0.153	-	0.207	-
57	-	0.183	-	0.251	-	0.380	-	0.468	-	0.162	-	0.247	-	0.166	-	0.248
58	0.164	-	0.211	-	0.342	-	0.391	-	0.159	-	0.202	-	0.151	-	0.207	-
59	-	0.182	-	0.253	-	0.377	-	0.472	-	-	-	0.249	-	-	-	-
60	0.162	-	0.211	-	0.338	-	0.392	-	0.157	-	0.202	-	0.150	-	0.207	-

27

Table B.3: Einstein coefficients A of laser transitions of '628' CO_2, s^{-1}

	Regular				Sequence				Hot-e				Hot-f			
J	10P	10R	9P	9R	10P	10R	9P	9R	10P	10R	9P	9R	10P	10R	9P	9R
0	-	0.100	-	0.192	-	-	-	-	-	0.089	-	0.162	-	0.089	-	0.162
1	0.298	0.120	0.574	0.231	-	-	-	0.463	0.148	0.113	0.268	0.206	0.148	0.113	0.268	0.206
2	0.199	0.128	0.382	0.248	-	-	-	0.481	0.158	0.123	0.285	0.225	0.157	0.124	0.285	0.225
3	0.179	0.133	0.343	0.257	-	-	-	0.493	0.158	0.129	0.286	0.236	0.158	0.130	0.286	0.236
4	0.170	0.136	0.326	0.263	-	0.287	0.642	0.501	0.157	0.133	0.284	0.244	0.157	0.133	0.284	0.243
5	0.165	0.139	0.317	0.268	0.348	0.292	0.611	0.508	0.156	0.136	0.282	0.249	0.156	0.136	0.282	0.248
6	0.162	0.140	0.311	0.271	0.341	0.295	0.593	0.513	0.155	0.137	0.280	0.252	0.155	0.138	0.280	0.252
7	0.159	0.141	0.306	0.274	0.336	0.298	0.581	0.517	0.154	0.139	0.278	0.255	0.154	0.139	0.279	0.255
8	0.158	0.142	0.303	0.276	0.332	0.300	0.573	0.521	0.154	0.140	0.277	0.258	0.153	0.140	0.277	0.257
9	0.156	0.143	0.300	0.278	0.329	0.302	0.567	0.524	0.153	0.141	0.277	0.260	0.153	0.141	0.277	0.259
10	0.155	0.144	0.298	0.280	0.327	0.303	0.562	0.527	0.152	0.141	0.275	0.262	0.152	0.141	0.276	0.261
11	0.154	0.144	0.296	0.282	0.324	0.304	0.558	0.530	0.152	0.142	0.274	0.263	0.151	0.142	0.275	0.263
12	0.153	0.145	0.295	0.283	0.323	0.305	0.555	0.532	0.151	0.142	0.273	0.265	0.151	0.143	0.273	0.263
13	0.152	0.145	0.294	0.284	0.321	0.306	0.552	0.534	0.151	0.143	0.272	0.266	0.150	0.143	0.273	0.264
14	0.152	0.145	0.292	0.285	0.319	0.307	0.549	0.537	0.150	0.143	0.271	0.267	0.150	0.143	0.272	0.265
15	0.151	0.146	0.291	0.287	0.318	0.307	0.547	0.538	0.150	0.143	0.270	0.268	0.149	0.144	0.271	0.267
16	0.150	0.146	0.290	0.288	0.316	0.308	0.545	0.538	0.150	0.143	0.269	0.269	0.149	0.144	0.270	0.268
17	0.150	0.146	0.289	0.289	0.315	0.308	0.543	0.541	0.149	0.144	0.268	0.270	0.148	0.144	0.269	0.269
18	0.149	0.146	0.289	0.290	0.314	0.309	0.542	0.542	0.149	0.144	0.268	0.271	0.148	0.145	0.269	0.270
19	0.148	0.146	0.288	0.291	0.312	0.309	0.540	0.544	0.148	0.144	0.267	0.272	0.147	0.145	0.268	0.271
20	0.148	0.146	0.288	0.291	0.311	0.309	0.539	0.546	0.148	0.144	0.266	0.273	0.147	0.145	0.267	0.272
21	0.147	0.147	0.287	0.292	0.310	0.309	0.538	0.548	0.148	0.144	0.266	0.274	0.146	0.145	0.267	0.272
22	0.147	0.147	0.286	0.293	0.309	0.309	0.537	0.550	0.147	0.144	0.265	0.275	0.146	0.145	0.266	0.273
23	0.146	0.147	0.286	0.294	0.308	0.309	0.535	0.551	0.147	0.144	0.264	0.275	0.145	0.145	0.266	0.274
24	0.146	0.147	0.285	0.295	0.307	0.309	0.534	0.553	0.147	0.144	0.264	0.276	0.145	0.145	0.265	0.275
25	0.145	0.146	0.285	0.296	0.305	0.309	0.533	0.555	0.146	0.144	0.263	0.277	0.144	0.145	0.265	0.276
26	0.144	0.146	0.284	0.297	0.304	0.309	0.532	0.556	0.146	0.144	0.263	0.278	0.144	0.145	0.264	0.276
27	0.144	0.146	0.284	0.298	0.303	0.309	0.532	0.558	0.145	0.144	0.262	0.279	0.143	0.145	0.264	0.277
28	0.143	0.146	0.283	0.298	0.302	0.308	0.531	0.559	0.145	0.144	0.262	0.279	0.143	0.145	0.263	0.278
29	0.143	0.146	0.283	0.299	0.301	0.308	0.530	0.561	0.145	0.144	0.261	0.280	0.142	0.145	0.263	0.279
30	0.142	0.146	0.282	0.300	0.300	0.308	0.529	0.563	0.144	0.144	0.261	0.281	0.142	0.145	0.263	0.280
31	0.142	0.146	0.282	0.301	0.298	-	0.528	0.564	0.144	0.143	0.260	0.282	0.141	0.145	0.262	0.281
32	0.141	0.146	0.282	0.302	0.297	-	0.528	0.566	0.144	0.143	0.260	0.282	0.141	0.145	0.262	0.282
33	0.141	0.146	0.281	0.302	-	-	0.527	0.568	0.143	0.143	0.259	0.283	0.140	0.145	0.261	0.282
34	0.140	0.145	0.281	0.303	-	-	0.526	0.569	0.143	0.143	0.259	0.284	0.140	0.144	0.261	0.283
35	0.139	0.145	0.280	0.304	-	-	0.526	0.570	0.143	0.143	0.259	0.284	0.140	0.144	0.261	0.284
36	0.139	0.145	0.280	0.305	-	-	0.525	0.572	0.142	0.143	0.258	0.285	0.139	0.144	0.260	0.284
37	0.138	0.145	0.280	0.306	-	-	0.525	0.574	0.142	0.142	0.258	0.286	0.139	0.144	0.260	0.285
38	0.138	0.144	0.279	0.307	-	-	0.524	0.575	0.142	0.142	0.257	0.287	0.138	0.144	0.260	0.286
39	0.137	0.144	0.279	0.307	-	-	0.523	0.577	0.141	0.142	0.257	0.287	0.138	0.144	0.259	0.286
40	0.136	0.144	0.279	0.308	-	-	0.523	0.579	0.141	0.142	0.256	0.288	0.137	0.144	0.259	0.287
41	0.136	0.143	0.279	0.309	-	-	0.522	-	0.140	0.141	0.256	0.289	0.137	0.143	0.259	0.288
42	0.135	0.143	0.278	0.310	-	-	-	-	0.140	0.141	0.256	0.290	0.136	0.143	0.258	0.288
43	0.134	0.143	0.278	0.311	-	-	-	-	0.139	0.141	0.255	0.290	0.136	0.143	0.258	0.289
44	0.134	0.142	0.277	0.312	-	-	-	-	0.139	0.141	0.255	0.291	0.135	0.143	0.258	0.290
45	0.133	0.142	0.277	0.312	-	-	-	-	0.139	0.140	0.255	0.292	0.135	0.142	0.258	0.291
46	0.133	0.142	0.277	0.313	-	-	-	-	0.138	0.140	0.254	0.292	0.134	0.142	0.257	0.291
47	0.132	0.141	0.277	0.314	-	-	-	-	0.138	0.140	0.254	0.293	0.133	0.142	0.257	0.292
48	0.131	0.141	0.277	0.315	-	-	-	-	0.137	0.139	0.254	0.294	0.133	0.141	0.257	0.293
49	0.131	0.140	0.276	0.316	-	-	-	-	0.137	0.139	0.253	0.295	0.132	0.141	0.257	0.294
50	0.130	0.140	0.276	0.317	-	-	-	-	0.136	0.139	0.253	0.295	0.132	0.141	0.256	0.294
51	0.130	0.140	0.276	0.318	-	-	-	-	0.136	0.138	0.253	0.296	0.131	0.140	0.256	0.295
52	0.129	0.139	0.276	0.318	-	-	-	-	0.135	0.138	0.252	0.297	0.131	0.140	0.256	0.296
53	0.128	0.139	0.276	0.319	-	-	-	-	0.135	0.138	0.252	0.298	0.130	0.140	0.256	0.297
54	0.128	0.138	0.275	0.320	-	-	-	-	0.134	0.137	0.252	0.298	0.129	0.139	0.256	0.297
55	0.127	0.138	0.275	0.321	-	-	-	-	0.134	0.137	0.251	0.299	0.129	0.139	0.255	0.298
56	0.126	0.138	0.275	0.322	-	-	-	-	0.133	0.136	0.251	0.300	0.128	0.138	0.255	0.299
57	0.126	0.137	0.275	0.323	-	-	-	-	0.133	0.136	0.251	0.301	0.128	0.138	0.255	0.300
58	0.125	0.137	0.275	0.324	-	-	-	-	0.132	0.136	0.251	0.301	0.127	0.137	0.255	0.301
59	0.124	0.136	0.275	0.325	-	-	-	-	0.132	0.135	0.250	-	0.126	0.137	0.255	-
60	0.123	-	0.275	-	-	-	-	-	0.131	0.135	0.250	-	0.125	-	0.254	-

28

Table B.4: Einstein coefficients A of laser transitions of '828' CO_2, s^{-1}

J	Regular				Sequence				Hot-e				Hot-f			
	10P	10R	9P	9R	10P	10R	9P	9R	10P	10R	9P	9R	10P	10R	9P	9R
0	-	-	-	-	-	-	-	-	-	-	-	-	-	-	-	-
1	-	0.073	-	0.234	-	-	-	-	-	-	-	0.192	-	-	-	0.243
2	0.146	0.094	0.466	0.301	-	-	-	-	-	-	0.337	0.267	-	-	0.318	0.280
3	-	-	-	-	-	-	-	-	-	-	-	-	-	-	-	-
4	0.125	0.100	0.398	0.321	-	-	-	-	-	-	0.336	0.288	-	-	0.338	0.294
5	-	-	-	-	-	-	-	-	-	-	-	-	-	-	-	-
6	0.119	0.103	0.379	0.330	-	-	-	-	0.128	0.108	0.332	0.298	0.127	0.105	0.334	0.301
7	-	-	-	-	-	-	-	-	-	-	-	-	-	-	-	-
8	0.116	0.104	0.368	0.337	-	-	-	-	0.127	0.112	0.328	0.304	0.125	0.111	0.330	0.307
9	-	-	-	-	-	-	-	-	-	-	-	-	-	-	-	-
10	0.114	0.105	0.363	0.340	-	-	-	-	0.125	0.114	0.325	0.309	0.124	0.113	0.327	0.310
11	-	-	-	-	-	-	-	-	-	-	-	-	-	-	-	-
12	0.112	0.106	0.360	0.343	-	-	-	-	0.124	0.115	0.322	0.312	0.123	0.115	0.324	0.313
13	-	-	-	-	-	-	-	-	-	-	-	-	-	-	-	-
14	0.111	0.106	0.356	0.347	-	-	-	-	0.123	0.116	0.320	0.315	0.122	0.116	0.322	0.317
15	-	-	-	-	-	-	-	-	-	-	-	-	-	-	-	-
16	0.110	0.107	0.353	0.349	-	-	-	-	0.122	0.116	0.318	0.318	0.121	0.117	0.320	0.318
17	-	-	-	-	-	-	-	-	-	-	-	-	-	-	-	-
18	0.109	0.107	0.351	0.351	-	-	-	-	0.122	0.117	0.317	0.319	0.120	0.117	0.318	0.320
19	-	-	-	-	-	-	-	-	-	-	-	-	-	-	-	-
20	0.108	0.107	0.349	0.353	-	-	-	-	0.121	0.117	0.315	0.322	0.119	0.118	0.317	0.322
21	-	-	-	-	-	-	-	-	-	-	-	-	-	-	-	-
22	0.108	0.107	0.348	0.355	-	-	-	-	0.120	0.117	0.314	0.323	0.119	0.118	0.315	0.324
23	-	-	-	-	-	-	-	-	-	-	-	-	-	-	-	-
24	0.107	0.107	0.346	0.357	-	-	-	-	0.120	0.117	0.312	0.325	0.118	0.118	0.314	0.325
25	-	-	-	-	-	-	-	-	-	-	-	-	-	-	-	-
26	0.106	0.107	0.346	0.359	-	-	-	-	0.119	0.117	0.311	0.327	0.117	0.118	0.313	0.327
27	-	-	-	-	-	-	-	-	-	-	-	-	-	-	-	-
28	0.105	0.107	0.343	0.360	-	-	-	-	0.119	0.117	0.310	0.328	0.116	0.118	0.312	0.328
29	-	-	-	-	-	-	-	-	-	-	-	-	-	-	-	-
30	0.105	0.107	0.342	0.362	-	-	-	-	0.118	0.117	0.309	0.330	0.116	0.118	0.311	0.330
31	-	-	-	-	-	-	-	-	-	-	-	-	-	-	-	-
32	0.104	0.106	0.341	0.364	-	-	-	-	0.117	0.116	0.307	0.332	0.115	0.118	0.310	0.332
33	-	-	-	-	-	-	-	-	-	-	-	-	-	-	-	-
34	0.103	0.106	0.340	0.365	-	-	-	-	0.117	-	0.307	0.333	0.114	-	0.309	0.333
35	-	-	-	-	-	-	-	-	-	-	-	-	-	-	-	-
36	0.102	0.106	0.340	0.367	-	-	-	-	-	-	0.305	0.334	-	-	0.308	0.334
37	-	-	-	-	-	-	-	-	-	-	-	-	-	-	-	-
38	0.101	0.105	0.339	0.369	-	-	-	-	-	-	0.305	0.336	-	-	0.307	0.336
39	-	-	-	-	-	-	-	-	-	-	-	-	-	-	-	-
40	0.100	0.104	0.338	0.370	-	-	-	-	-	-	0.304	0.337	-	-	0.306	0.337
41	-	-	-	-	-	-	-	-	-	-	-	-	-	-	-	-
42	0.100	0.104	0.337	0.372	-	-	-	-	-	-	0.302	0.339	-	-	0.305	0.338
43	-	-	-	-	-	-	-	-	-	-	-	-	-	-	-	-
44	0.098	0.104	0.336	0.373	-	-	-	-	-	-	0.301	0.340	-	-	0.304	0.342
45	-	-	-	-	-	-	-	-	-	-	-	-	-	-	-	-
46	0.097	0.103	0.335	0.375	-	-	-	-	-	-	0.300	0.343	-	-	0.305	-
47	-	-	-	-	-	-	-	-	-	-	-	-	-	-	-	-
48	0.096	0.103	0.335	0.376	-	-	-	-	-	-	-	-	-	-	-	-
49	-	-	-	-	-	-	-	-	-	-	-	-	-	-	-	-
50	0.095	0.102	0.333	0.378	-	-	-	-	-	-	-	-	-	-	-	-
51	-	-	-	-	-	-	-	-	-	-	-	-	-	-	-	-
52	0.095	0.101	0.333	0.378	-	-	-	-	-	-	-	-	-	-	-	-
53	-	-	-	-	-	-	-	-	-	-	-	-	-	-	-	-
54	0.093	0.100	0.332	0.381	-	-	-	-	-	-	-	-	-	-	-	-
55	-	-	-	-	-	-	-	-	-	-	-	-	-	-	-	-
56	0.092	0.099	0.331	0.382	-	-	-	-	-	-	-	-	-	-	-	-
57	-	-	-	-	-	-	-	-	-	-	-	-	-	-	-	-
58	-	-	0.331	0.384	-	-	-	-	-	-	-	-	-	-	-	-
59	-	-	-	-	-	-	-	-	-	-	-	-	-	-	-	-
60	-	-	0.331	-	-	-	-	-	-	-	-	-	-	-	-	-

29

Table B.5: Einstein coefficients A of laser transitions of '636' CO_2, s^{-1}

J	Regular 10P	Regular 10R	Regular 9P	Regular 9R	Sequence 10P	Sequence 10R	Sequence 9P	Sequence 9R	Hot-e 10P	Hot-e 10R	Hot-e 9P	Hot-e 9R	Hot-f 10P	Hot-f 10R	Hot-f 9P	Hot-f 9R
0	-	0.138	-	0.072	-	-	-	-	-	-	-	-	-	-	-	-
1	-	-	-	-	0.833	0.335	-	0.158	0.188	-	-	-	-	0.134	-	0.095
2	0.276	0.178	0.143	0.093	-	-	-	-	-	0.106	-	0.075	0.175	-	0.124	-
3	-	-	-	-	0.500	0.374	0.235	0.176	0.187	-	0.132	-	-	0.154	-	0.109
4	0.237	0.190	0.122	0.099	-	-	-	-	-	0.147	-	0.105	0.188	-	0.132	-
5	-	-	-	-	0.462	0.389	0.217	0.184	0.185	-	0.131	-	-	0.162	-	0.115
6	0.225	0.195	0.116	0.102	-	-	-	-	-	0.158	-	0.113	0.185	-	0.130	-
7	-	-	-	-	0.447	0.397	0.209	0.188	0.183	-	0.129	-	-	0.166	-	0.118
8	0.219	0.198	0.113	0.104	-	-	-	-	-	0.164	-	0.117	0.183	-	0.129	-
9	-	-	-	-	0.438	0.403	0.205	0.191	0.181	-	0.128	-	-	0.168	-	0.121
10	0.215	0.200	0.111	0.105	-	-	-	-	-	0.167	-	0.120	0.181	-	0.127	-
11	-	-	-	-	0.431	0.406	0.202	0.194	0.180	-	0.126	-	-	0.171	-	0.122
12	0.213	0.202	0.110	0.107	-	-	-	-	-	0.169	-	0.121	0.179	-	0.126	-
13	-	-	-	-	0.428	0.409	0.200	0.196	0.179	-	0.125	-	-	0.171	-	0.123
14	0.210	0.203	0.109	0.108	-	-	-	-	-	0.170	-	0.124	0.179	-	0.125	-
15	-	-	-	-	0.422	0.413	0.199	0.198	0.178	-	0.124	-	-	0.173	-	0.124
16	0.209	0.204	0.108	0.109	-	-	-	-	-	0.170	-	0.125	0.176	-	0.125	-
17	-	-	-	-	0.419	0.414	0.198	0.200	0.176	-	0.124	-	-	0.173	-	0.126
18	0.207	0.204	0.108	0.110	-	-	-	-	-	0.171	-	0.125	0.176	-	0.124	-
19	-	-	-	-	0.415	0.415	0.197	0.201	0.177	-	0.123	-	-	0.174	-	0.127
20	0.206	0.205	0.107	0.111	-	-	-	-	-	0.172	-	0.127	0.174	-	0.124	-
21	-	-	-	-	0.414	0.416	0.196	0.203	0.175	-	0.122	-	-	0.174	-	0.127
22	0.205	0.206	0.107	0.112	-	-	-	-	-	0.171	-	0.128	0.174	-	0.123	-
23	-	-	-	-	0.411	0.416	0.195	0.205	0.174	-	0.121	-	-	0.174	-	0.129
24	0.203	0.206	0.106	0.112	-	-	-	-	-	0.172	-	0.128	0.172	-	0.122	-
25	-	-	-	-	0.409	0.417	0.195	0.206	0.174	-	0.121	-	-	0.174	-	0.130
26	0.202	0.207	0.106	0.113	-	-	-	-	-	0.172	-	0.130	0.171	-	0.122	-
27	-	-	-	-	0.406	0.418	0.194	0.208	0.173	-	0.120	-	-	0.174	-	0.131
28	0.201	0.207	0.106	0.114	-	-	-	-	-	0.172	-	0.131	0.171	-	0.122	-
29	-	-	-	-	0.403	0.418	0.194	0.210	0.172	-	0.120	-	-	0.175	-	0.132
30	0.199	0.207	0.105	0.114	-	-	-	-	-	0.172	-	0.132	0.169	-	0.121	-
31	-	-	-	-	0.401	0.419	0.193	0.212	0.171	-	0.119	-	-	0.174	-	0.132
32	0.197	0.207	0.105	0.116	-	-	-	-	-	0.172	-	0.133	0.169	-	0.121	-
33	-	-	-	-	0.398	0.419	0.193	0.214	0.170	-	0.119	-	-	0.174	-	0.133
34	0.197	0.206	0.105	0.117	-	-	-	-	-	0.172	-	0.134	0.168	-	0.121	-
35	-	-	-	-	0.396	0.418	0.193	0.215	0.170	-	0.118	-	-	0.174	-	0.134
36	0.196	0.207	0.105	0.118	-	-	-	-	-	0.171	-	0.135	0.166	-	0.120	-
37	-	-	-	-	0.394	0.418	0.193	0.217	0.169	-	0.118	-	-	0.174	-	0.135
38	0.194	0.206	0.105	0.119	-	-	-	-	-	0.171	-	0.136	0.165	-	0.120	-
39	-	-	-	-	0.390	0.419	0.193	0.219	0.168	-	0.117	-	-	0.173	-	0.136
40	0.193	0.206	0.105	0.120	-	-	-	-	-	0.170	-	0.136	0.164	-	0.120	-
41	-	-	-	-	0.389	0.417	0.192	0.220	0.167	-	0.117	-	-	0.173	-	0.137
42	0.192	0.206	0.105	0.121	-	-	-	-	-	0.170	-	0.138	0.163	-	0.120	-
43	-	-	-	-	0.385	0.418	-	-	0.166	-	0.117	-	-	0.173	-	0.138
44	0.190	0.206	0.105	0.122	-	-	-	-	-	0.170	-	0.139	0.163	-	0.120	-
45	-	-	-	-	-	-	-	-	0.165	-	0.116	-	-	0.172	-	0.139
46	0.189	0.205	0.105	0.123	-	-	-	-	-	0.169	-	0.139	0.161	-	0.120	-
47	-	-	-	-	-	-	-	-	0.164	-	0.116	-	-	0.172	-	0.140
48	0.187	0.204	0.105	0.123	-	-	-	-	-	0.169	-	0.140	0.160	-	0.119	-
49	-	-	-	-	-	-	-	-	0.163	-	0.116	-	-	0.171	-	0.141
50	0.186	0.203	0.105	0.125	-	-	-	-	-	0.168	-	0.141	0.159	-	0.120	-
51	-	-	-	-	-	-	-	-	0.163	-	0.116	-	-	0.170	-	0.142
52	0.185	0.203	0.105	0.126	-	-	-	-	-	0.167	-	0.142	0.158	-	0.119	-
53	-	-	-	-	-	-	-	-	0.162	-	0.115	-	-	0.170	-	0.143
54	0.183	0.203	0.105	0.127	-	-	-	-	-	0.166	-	0.143	0.157	-	0.119	-
55	-	-	-	-	-	-	-	-	0.161	-	-	-	-	0.169	-	0.145
56	0.182	0.202	0.105	0.128	-	-	-	-	-	0.165	-	0.145	0.155	-	0.119	-
57	-	-	-	-	-	-	-	-	0.160	-	-	-	-	-	-	0.146
58	0.180	0.201	0.105	0.129	-	-	-	-	-	0.165	-	0.146	0.154	-	0.119	-
59	-	-	-	-	-	-	-	-	-	-	-	-	-	-	-	-
60	0.178	-	0.105	-	-	-	-	-	-	-	-	0.147	0.153	-	0.119	-

Table B.6: Einstein coefficients A of laser transitions of '638' CO_2, s^{-1}

J	Regular				Sequence				Hot-e				Hot-f			
	10P	10R	9P	9R	10P	10R	9P	9R	10P	10R	9P	9R	10P	10R	9P	9R
0	-	0.117	-	0.106	-	-	-	-	-	-	-	-	-	-	-	-
1	0.350	0.141	0.315	0.127	-	-	-	-	-	0.093	-	0.098	-	0.093	-	0.098
2	0.233	0.151	0.210	0.136	-	-	-	-	0.155	0.118	0.163	0.125	0.155	0.118	0.163	0.125
3	0.210	0.157	0.189	0.141	-	-	-	-	0.165	0.129	0.173	0.137	0.165	0.130	0.173	0.137
4	0.199	0.160	0.179	0.145	-	-	-	-	0.166	0.136	0.174	0.144	0.165	0.136	0.174	0.144
5	0.194	0.163	0.174	0.147	-	-	-	-	0.165	0.139	0.172	0.148	0.164	0.140	0.173	0.148
6	0.190	0.165	0.171	0.149	-	-	-	-	0.164	0.142	0.171	0.151	0.163	0.142	0.171	0.151
7	0.187	0.166	0.168	0.151	-	-	-	-	0.163	0.144	0.170	0.154	0.162	0.144	0.170	0.153
8	0.185	0.167	0.166	0.152	-	-	-	-	0.162	0.145	0.169	0.155	0.161	0.146	0.169	0.155
9	0.183	0.168	0.165	0.153	-	-	-	-	0.161	0.147	0.168	0.157	0.160	0.147	0.168	0.157
10	0.182	0.169	0.164	0.154	-	-	-	-	0.160	0.147	0.167	0.158	0.159	0.148	0.167	0.158
11	0.181	0.170	0.163	0.155	-	-	-	-	0.159	0.148	0.166	0.159	0.159	0.149	0.167	0.159
12	0.180	0.170	0.162	0.156	-	-	-	-	0.159	0.149	0.166	0.160	0.158	0.150	0.166	0.160
13	0.179	0.171	0.161	0.157	-	-	-	-	0.158	0.149	0.165	0.161	0.157	0.150	0.165	0.161
14	0.178	0.171	0.161	0.158	-	-	-	-	0.158	0.150	0.164	0.162	0.157	0.151	0.165	0.162
15	0.177	0.172	0.160	0.158	-	-	-	-	0.157	0.150	0.164	0.163	0.156	0.151	0.164	0.163
16	0.176	0.172	0.160	0.159	-	-	-	-	0.157	0.150	0.163	0.164	0.156	0.151	0.164	0.163
17	0.176	0.172	0.159	0.160	-	-	-	-	0.156	0.151	0.163	0.164	0.155	0.152	0.164	0.164
18	0.175	0.173	0.159	0.160	-	-	-	-	0.156	0.151	0.162	0.165	0.155	0.152	0.163	0.165
19	0.174	0.173	0.158	0.161	-	-	-	-	0.156	0.151	0.162	0.166	0.154	0.152	0.163	0.165
20	0.174	0.173	0.158	0.161	-	-	-	-	0.155	0.151	0.161	0.166	0.154	0.152	0.162	0.166
21	0.173	0.173	0.158	0.162	-	-	-	-	0.155	0.151	0.161	0.167	0.153	0.153	0.162	0.166
22	0.173	0.173	0.157	0.162	-	-	-	-	0.154	0.151	0.161	0.167	0.153	0.153	0.162	0.167
23	0.172	0.173	0.157	0.163	-	-	-	-	0.154	0.151	0.160	0.168	0.152	0.153	0.161	0.168
24	0.171	0.173	0.157	0.164	-	-	-	-	0.154	0.151	0.160	0.169	0.152	0.153	0.161	0.168
25	0.171	0.173	0.157	0.164	-	-	-	-	0.153	0.151	0.160	0.169	0.151	0.153	0.161	0.169
26	0.170	0.173	0.156	0.165	-	-	-	-	0.153	0.152	0.159	0.170	0.151	0.153	0.161	0.169
27	0.170	0.173	0.156	0.165	-	-	-	-	0.153	0.152	0.159	0.170	0.150	0.153	0.160	0.170
28	0.169	0.173	0.156	0.166	-	-	-	-	0.152	0.151	0.159	0.171	0.150	0.153	0.160	0.170
29	0.168	0.173	0.156	0.166	-	-	-	-	0.152	0.151	0.158	0.171	0.149	0.153	0.160	0.171
30	0.168	0.173	0.156	0.167	-	-	-	-	0.151	0.151	0.158	0.172	0.149	0.153	0.160	0.171
31	0.167	0.173	0.155	0.168	-	-	-	-	0.151	0.151	0.158	0.172	0.148	0.153	0.160	0.172
32	0.167	0.173	0.155	0.168	-	-	-	-	0.151	0.151	0.157	0.173	0.148	0.153	0.159	0.172
33	0.166	0.173	0.155	0.169	-	-	-	-	0.150	0.151	0.157	0.173	0.147	0.153	0.159	0.173
34	0.166	0.173	0.155	0.169	-	-	-	-	0.150	0.151	0.157	0.174	0.147	0.153	0.159	0.173
35	0.165	0.173	0.155	0.170	-	-	-	-	0.149	0.151	0.157	0.175	0.146	0.153	0.159	0.174
36	0.164	0.173	0.155	0.171	-	-	-	-	0.149	0.151	0.156	0.175	0.146	0.153	0.159	0.175
37	0.164	0.173	0.155	0.171	-	-	-	-	0.149	0.151	0.156	0.176	0.146	0.152	0.158	0.175
38	0.163	0.172	0.155	0.172	-	-	-	-	0.148	0.150	0.156	0.176	0.145	0.152	0.158	0.176
39	0.162	0.172	0.155	0.172	-	-	-	-	0.148	0.150	0.156	0.177	0.145	0.152	0.158	0.176
40	0.162	0.172	0.154	0.173	-	-	-	-	0.148	0.150	0.156	0.177	0.144	0.152	0.158	0.177
41	0.161	0.172	0.154	0.174	-	-	-	-	0.147	0.150	0.155	0.178	0.144	0.152	0.158	0.177
42	0.161	0.172	0.154	0.174	-	-	-	-	0.147	0.150	0.155	0.178	0.143	0.152	0.158	0.178
43	0.160	0.171	0.154	0.175	-	-	-	-	0.146	0.149	0.155	0.179	0.142	0.151	0.158	0.178
44	0.159	0.171	0.154	0.175	-	-	-	-	0.146	0.149	0.155	0.179	0.142	0.151	0.158	0.179
45	0.159	0.171	0.154	0.176	-	-	-	-	0.145	0.149	0.154	0.180	0.141	0.151	0.157	0.179
46	0.158	0.170	0.154	0.177	-	-	-	-	0.145	0.149	0.154	0.181	0.141	0.151	0.157	0.180
47	0.157	0.170	0.154	0.177	-	-	-	-	0.145	0.148	0.154	0.181	0.140	0.150	0.157	0.181
48	0.157	0.170	0.154	0.178	-	-	-	-	0.144	0.148	0.154	0.182	0.140	0.150	0.157	0.181
49	0.156	0.169	0.154	0.179	-	-	-	-	0.144	0.148	0.154	0.182	0.139	0.150	0.157	0.182
50	0.155	0.169	0.154	0.179	-	-	-	-	0.143	0.147	0.154	0.183	0.139	0.150	0.157	0.182
51	0.154	0.169	0.154	0.180	-	-	-	-	0.143	0.147	0.154	0.183	0.138	0.149	0.157	0.183
52	0.154	0.168	0.154	0.181	-	-	-	-	0.142	0.147	0.153	0.184	0.138	0.149	0.157	0.184
53	0.153	0.168	0.154	0.181	-	-	-	-	0.142	0.147	0.153	0.184	0.137	0.149	0.157	0.184
54	0.152	0.167	0.154	0.182	-	-	-	-	0.142	0.146	0.153	0.185	0.136	0.148	0.157	0.185
55	0.152	0.167	0.154	0.183	-	-	-	-	0.141	-	0.153	0.186	0.136	-	0.157	0.185
56	0.151	0.167	0.154	0.184	-	-	-	-	-	-	0.153	0.186	-	-	0.157	0.186
57	0.150	0.166	0.154	0.184	-	-	-	-	-	-	0.153	0.187	-	-	0.157	0.187
58	0.149	0.166	0.154	0.185	-	-	-	-	-	-	-	-	-	-	-	-
59	0.149	0.165	0.154	0.186	-	-	-	-	-	-	-	-	-	-	-	-
60	0.148	-	0.155	-	-	-	-	-	-	-	-	-	-	-	-	-

31

Table B.7: Einstein coefficients A of laser transitions of '838' CO_2, s^{-1}

J	Regular 10P	Regular 10R	Regular 9P	Regular 9R	Sequence 10P	Sequence 10R	Sequence 9P	Sequence 9R	Hot-e 10P	Hot-e 10R	Hot-e 9P	Hot-e 9R	Hot-f 10P	Hot-f 10R	Hot-f 9P	Hot-f 9R
0	-	-	-	-	-	-	-	-	-	-	-	-	-	-	-	-
1	-	-	-	-	-	-	-	-	-	-	-	-	-	-	-	-
2	-	-	-	-	-	-	-	-	-	-	-	-	-	-	-	-
3	-	-	-	-	-	-	-	-	-	-	-	-	-	-	-	-
4	-	-	-	-	-	-	-	-	-	-	-	-	-	-	-	-
5	-	-	-	-	-	-	-	-	-	-	-	-	-	-	-	-
6	0.233	0.203	0.233	0.203	-	-	-	-	-	-	-	-	-	-	-	-
7	-	-	-	-	-	-	-	-	-	-	-	-	-	-	-	-
8	0.227	0.206	0.227	0.206	-	-	-	-	-	-	-	-	-	-	-	-
9	-	-	-	-	-	-	-	-	-	-	-	-	-	-	-	-
10	0.223	0.209	0.223	0.209	-	-	-	-	-	-	-	-	-	-	-	-
11	-	-	-	-	-	-	-	-	-	-	-	-	-	-	-	-
12	0.220	0.211	0.220	0.211	-	-	-	-	-	-	-	-	-	-	-	-
13	-	-	-	-	-	-	-	-	-	-	-	-	-	-	-	-
14	0.219	0.213	0.219	0.213	-	-	-	-	-	-	-	-	-	-	-	-
15	-	-	-	-	-	-	-	-	-	-	-	-	-	-	-	-
16	0.217	0.215	0.217	0.215	-	-	-	-	-	-	-	-	-	-	-	-
17	-	-	-	-	-	-	-	-	-	-	-	-	-	-	-	-
18	0.216	0.217	0.216	0.217	-	-	-	-	-	-	-	-	-	-	-	-
19	-	-	-	-	-	-	-	-	-	-	-	-	-	-	-	-
20	0.215	0.219	0.215	0.219	-	-	-	-	-	-	-	-	-	-	-	-
21	-	-	-	-	-	-	-	-	-	-	-	-	-	-	-	-
22	0.214	0.219	0.214	0.219	-	-	-	-	-	-	-	-	-	-	-	-
23	-	-	-	-	-	-	-	-	-	-	-	-	-	-	-	-
24	0.214	0.221	0.214	0.221	-	-	-	-	-	-	-	-	-	-	-	-
25	-	-	-	-	-	-	-	-	-	-	-	-	-	-	-	-
26	0.213	0.222	0.213	0.222	-	-	-	-	-	-	-	-	-	-	-	-
27	-	-	-	-	-	-	-	-	-	-	-	-	-	-	-	-
28	0.212	0.224	0.212	0.224	-	-	-	-	-	-	-	-	-	-	-	-
29	-	-	-	-	-	-	-	-	-	-	-	-	-	-	-	-
30	0.211	0.225	0.211	0.225	-	-	-	-	-	-	-	-	-	-	-	-
31	-	-	-	-	-	-	-	-	-	-	-	-	-	-	-	-
32	0.210	0.226	0.210	0.226	-	-	-	-	-	-	-	-	-	-	-	-
33	-	-	-	-	-	-	-	-	-	-	-	-	-	-	-	-
34	-	-	-	-	-	-	-	-	-	-	-	-	-	-	-	-
35	-	-	-	-	-	-	-	-	-	-	-	-	-	-	-	-
36	-	-	-	-	-	-	-	-	-	-	-	-	-	-	-	-
37	-	-	-	-	-	-	-	-	-	-	-	-	-	-	-	-
38	-	-	-	-	-	-	-	-	-	-	-	-	-	-	-	-
39	-	-	-	-	-	-	-	-	-	-	-	-	-	-	-	-
40	-	-	-	-	-	-	-	-	-	-	-	-	-	-	-	-
41	-	-	-	-	-	-	-	-	-	-	-	-	-	-	-	-
42	-	-	-	-	-	-	-	-	-	-	-	-	-	-	-	-
43	-	-	-	-	-	-	-	-	-	-	-	-	-	-	-	-
44	-	-	-	-	-	-	-	-	-	-	-	-	-	-	-	-
45	-	-	-	-	-	-	-	-	-	-	-	-	-	-	-	-
46	-	-	-	-	-	-	-	-	-	-	-	-	-	-	-	-
47	-	-	-	-	-	-	-	-	-	-	-	-	-	-	-	-
48	-	-	-	-	-	-	-	-	-	-	-	-	-	-	-	-
49	-	-	-	-	-	-	-	-	-	-	-	-	-	-	-	-
50	-	-	-	-	-	-	-	-	-	-	-	-	-	-	-	-
51	-	-	-	-	-	-	-	-	-	-	-	-	-	-	-	-
52	-	-	-	-	-	-	-	-	-	-	-	-	-	-	-	-
53	-	-	-	-	-	-	-	-	-	-	-	-	-	-	-	-
54	-	-	-	-	-	-	-	-	-	-	-	-	-	-	-	-
55	-	-	-	-	-	-	-	-	-	-	-	-	-	-	-	-
56	-	-	-	-	-	-	-	-	-	-	-	-	-	-	-	-
57	-	-	-	-	-	-	-	-	-	-	-	-	-	-	-	-
58	-	-	-	-	-	-	-	-	-	-	-	-	-	-	-	-
59	-	-	-	-	-	-	-	-	-	-	-	-	-	-	-	-
60	-	-	-	-	-	-	-	-	-	-	-	-	-	-	-	-

Appendix C

Properties of optical materials

The following expressions and values for linear (n_0) and nonlinear (n_2) refractive indexes are used in the program (wavelength λ in the dispersion formulas must be expressed in μm):

CdTe

$n_0 = \sqrt{1 + \frac{6.1977889\lambda^2}{\lambda^2 - 0.1005326} + \frac{3.2243821\lambda^2}{\lambda^2 - 5279.518}}$ [5]

$n_2 = -2.95 \times 10^{-13}$ cm^2/W at 1.06 μm [24]

GaAs

$n_0 = \sqrt{5.372514 + \frac{5.466742\lambda^2}{\lambda^2 - 0.4431307^2} + \frac{0.02429960\lambda^2}{\lambda^2 - 0.8746453^2} + \frac{1.957522\lambda^2}{\lambda^2 - 36.9166^2}}$ [25]

$n_2 = -3.26 \times 10^{-13}$ cm^2/W at 1.06 μm [24]

Ge

$n_0 = \sqrt{9.28156 + \frac{6.72880\lambda^2}{\lambda^2 - 0.44105} + \frac{0.21307\lambda^2}{\lambda^2 - 3870.1}}$ [1]

$n_2 = 2.83 \times 10^{-13}$ cm^2/W at 10.6 μm [24]

KCl

$n_0 = \sqrt{1.26486 + \frac{0.30523\lambda^2}{\lambda^2 - 0.100^2} + \frac{0.41620\lambda^2}{\lambda^2 - 0.131^2} + \frac{0.18870\lambda^2}{\lambda^2 - 0.162^2} + \frac{2.6200\lambda^2}{\lambda^2 - 70.42^2}}$ [16]

$n_2 = 5.6 \times 10^{-16}2$ cm^2/W at 1.06 μm [24]

NaCl

$n_0 = \sqrt{1.00055 + \frac{0.19800\lambda^2}{\lambda^2 - 0.050^2} + \frac{0.48398\lambda^2}{\lambda^2 - 0.100^2} + \frac{0.38696\lambda^2}{\lambda^2 - 0.128^2} + \frac{0.25998\lambda^2}{\lambda^2 - 0.158^2} + \frac{0.08796\lambda^2}{\lambda^2 - 40.50^2} + \frac{3.17064\lambda^2}{\lambda^2 - 60.98^2} + \frac{0.30038\lambda^2}{\lambda^2 - 120.34^2}}$ [16]

$n_2 = 4.38 \times 10^{-16}$ cm^2/W at 1.06 μm [24]

Si

$n_0 = 3.41983 + \frac{0.159906}{\lambda^2 - 0.028} - 0.123109 \left(\frac{1}{\lambda^2 - 0.028} \right)^2 + 1.26878 \times 10^{-6}\lambda^2 - 1.95104 \times 10^{-9}\lambda^4$ [6]

$n_2 = 1.0 \times 10^{-13}$ cm^2/W at 2.2 μm [3]

ZnSe

$$n_0 = \sqrt{1 + \frac{4.45813734\lambda^2}{\lambda^2 - 0.200859853^2} + \frac{0.467216334\lambda^2}{\lambda^2 - 0.391371166^2} + \frac{2.89566290\lambda^2}{\lambda^2 - 47.1362108^2}} \quad [26]$$

$n_2 = 2.87 \times 10^{-14}$ cm^2/W at 1.06 μm [24]

Air

Refractive index n_0 is calculated using Mathar's model [19]

$n_2 = 3 \times 10^{-19}$ cm^2/W at 10.6 μm

Appendix D

Selected formulas explained

Equation 3.4

Eq. 3.4 defines the fraction z_{jk} of discharge energy spent in inelastic collisions:

$$z_{jk} = 10^{16} \frac{y_j u_{jk} \omega_{jk}}{\left(\frac{\xi \mathcal{E}}{\mathcal{N}}\right) v_d}$$

where y_j[-] is the relative concentration of a component in the gas mixture, u_{jk}[eV] is the transferred energy per electron-molecule collision, collision rate constant ω_{jk}[cm$^3 \cdot$s^{-1}] divided by electron drift speed v_d[cm$\cdot$s^{-1}] is the collision cross-section ([cm^2]), $\mathcal{E}$[10^{-16}V$\cdot$cm^{-1}] is the electric field, ξ[eV$\cdot$V^{-1}] is the energy gained by electron moved across an electric potential difference of 1 V, and $\mathcal{N}$[cm^{-3}] is the total absolute concentration of the gas mixture.

The physical meaning of $\xi\mathcal{E}$ is the energy (in eV) gained by an electron after passing 1 cm in the electric field $\mathcal{E}$. By definition of electronvolt, $\xi = 1$ and is thus omitted in Eq. 3.4.

Pumping rate constants in equations 3.8 and 3.9

Pumping rate constant is the number of quanta added to a given vibrational mode per unit of time per molecule.

$$p_e = \frac{1}{E_v[\text{J}]} \times \frac{1}{N[\text{cm}^{-3}]n[\text{-}]y[\text{-}]} \times q[\text{-}]W[\text{J} \cdot \text{s}^{-1} \cdot \text{cm}^{-3}]$$

where E_v is the energy of the vibrational quanta: 4.665e-20 J (2349 cm^{-1}) for ν_3 mode of CO_2 (and roughly same for N_2 vibration), and 1.325e-20 J (667 cm^{-1}) for ν_2 mode; N=2.7e19 cm^{-3} is the density of gas molecules under normal conditions (1 bar, 273 K); q is the fraction of discharge energy deposited in the corresponding vibration; n is the correction factor for molecular density at the conditions different from 'normal'; y is the relative concentration of the gas in the mixture; W is the discharge power density.

Combining the constants and switching to kW/cm^3 for power density and μs^{-1} for the rate constants we get the formulas given in the model description:

$$p_{e4} = 0.8 \times 10^{-3} \frac{q_4}{ny_2} W(t); \quad p_{e3} = 0.8 \times 10^{-3} \frac{q_3}{ny_1} W(t); \quad p_{e2} = 2.8 \times 10^{-3} \frac{q_2}{ny_1} W(t);$$

35

Bibliography

[1]   N. P. Barnes and M. S. Piltch. "Temperature-dependent Sellmeier coefficients and nonlinear optics average power limit for germanium". In: *J. Opt. Soc. Am.* 69 (1979), pp. 178–180. DOI: 10.1364/JOSA.69.000178.

[2]   A. S. Biryukov et al. "Relaxation of the vibrational energy of the (00^01) level of the CO_2 molecule". In: *Sov. J. Exp. Theor. Phys.* 39 (1974), p. 610.

[3]   A. D. Bristow, N. Rotenberg, and H. M. van Driel. "Two-photon absorption and Kerr coefficients of silicon for 850–2200 nm". In: *Appl. Phys. Lett.* 90 (2007), p. 191104. DOI: 10.1063/1.2737359.

[4]   N. Chandra and P. G. Burke. "Rotational excitation cross sections for e^--N_2 scattering". In: *J. Phys. B: At. Mol. Phys.* 6 (1973), pp. 2355–2357. DOI: 10.1088/0022-3700/6/11/030.

[5]   A. G. DeBell et al. "Cryogenic refractive indices and temperature coefficients of cadmium telluride from 6 μm to 22 μm". In: *Appl. Opt.* 18 (1979), pp. 3114–3115. DOI: 10.1364/AO.18.003114.

[6]   D. F. Edwards and E. Ochoa. "Infrared refractive index of silicon". In: *Appl. Opt.* 19 (1980), pp. 4130–4131. DOI: 10.1364/AO.19.004130.

[7]   A. G. Engelhardt, A. V. Phelps, and C. G. Risk. "Determination of Momentum Transfer and Inelastic Collision Cross Sections for Electrons in Nitrogen Using Transport Coefficients". In: *Phys. Rev.* 135 (1964), A1566–A1574. DOI: 10.1103/PhysRev.135.A1566.

[8]   B. J. Feldman. "Short-pulse multiline and multiband energy extraction in high-pressure CO_2-laser amplifiers". In: *IEEE J. Quant. Electron.* 9 (1973), pp. 1070–1078. DOI: 10.1109/JQE.1973.1077412.

[9]   C. Freed. "Status of CO_2 isotope lasers and their applications in tunable laser spectroscopy". In: *IEEE J. Quant. Electron.* 18 (1982), pp. 1220–1228. DOI: 10.1109/JQE.1982.1071680.

[10] L. S. Frost and A. V. Phelps. "Rotational Excitation and Momentum Transfer Cross Sections for Electrons in H_2 and N_2 from Transport Coefficients". In: *Phys. Rev.* 127 (1962), pp. 1621–1633. DOI: 10.1103/PhysRev.127.1621.

[11] I. E. Gordon et al. "The HITRAN2016 molecular spectroscopic database". In: *J. Quant. Spectr. Rad. Transfer* 203 (2017), pp. 3–69. DOI: 10.1016/j.jqsrt.2017.06.038.

[12] R. D. Hake and A. V. Phelps. "Momentum-transfer and inelastic-collision cross sections for electrons in O_2, CO, and CO_2". In: *Phys. Rev.* 158 (1967), pp. 70–84. DOI: 10.1103/PhysRev.158.70.

[13] R. C. Hilborn. "Einstein coefficients, cross sections, f values, dipole moments, and all that". In: *arXiv:physics/0202029* (2002).

[14] T. Holstein. "Energy distribution of electrons in high frequency gas discharges". In: *Phys. Rev.* 70 (1946), pp. 367–384. DOI: 10.1103/PhysRev.70.367.

[15] N. V. Karlov and Y. B. Konev. "High pressure pulsed CO_2 lasers". In: *Handbook on lasers*. Ed. by A. M. Prokhorov. Moscow: Sovetskoe Radio, 1978 (in Russian).

[16] H. H. Li. "Refractive index of alkali halides and its wavelength and temperature derivatives". In: *J. Phys. Chem. Ref. Data* 5 (1976), pp. 329–528. DOI: 10.1063/1.555536.

[17] J. J. Lowke, A. V. Phelps, and B. W. Irwin. "Predicted electron transport coefficients and operating characteristics of CO_2-N_2-He laser mixtures". In: *J. Appl. Phys.* 44 (1973), pp. 4664–4671. DOI: 10.1063/1.1662017.

[18] A.G. Maki et al. "Improved molecular constants and frequencies for the CO_2 laser from new high-J regular and hot-band frequency measurements". In: *J. Mol. Spectr.* 167 (1994), pp. 211–224. DOI: 10.1006/jmsp.1994.1227.

[19] R. J. Mathar. "Refractive index of humid air in the infrared: model fits". In: *J. Opt. A* 9 (2007), pp. 470–476. DOI: 10.1088/1464-4258/9/5/008.

[20] W. L. Nighan. "Electron energy distributions and collision rates in electrically excited N_2, CO, and CO_2". In: *Phys. Rev. A* 2 (1970), pp. 1989–2000. DOI: 10.1103/PhysRevA.2.1989.

[21] Y. D. Oksyuk. "Excitation of the rotational levels of diatomic molecules by electron impact in the adiabatic approximation". In: *Sov. J. Exp. Theor. Phys.* 22 (1966), pp. 873–881.

[22] A. V. Phelps. "Rotational and vibrational excitation of molecules by low-energy electrons". In: *Rev. Mod. Phys.* 40 (1968), pp. 399–410. DOI: 10.1103/RevModPhys.40.399.

[23] G. J. Schulz. "Vibrational excitation of nitrogen by electron impact". In: *Phys. Rev.* 125 (1962), pp. 229–232. DOI: 10.1103/PhysRev.125.229.

[24] M. Sheik-Bahae. "Dispersion of bound electron nonlinear refraction in solids". In: *IEEE J. Quant. Electron.* 27 (1991), pp. 1296–1309. DOI: 10.1109/3.89946.

[25] T. Skauli et al. "Improved dispersion relations for GaAs and applications to nonlinear optics". In: *J. Appl. Opt.* 94 (2003), pp. 6447–6455. DOI: 10.1063/1.1621740.

[26] B. Tatian. "Fitting refractive-index data with the Sellmeier dispersion formula". In: *Appl. Opt.* 23 (1984), pp. 4477–4485. DOI: 10.1364/AO.23.004477.

[27] R. L. Taylor and S. Bitterman. "Survey of Vibrational Relaxation Data for Processes Important in the CO_2-N_2 Laser System". In: *Rev. Mod. Phys.* 41 (1969), pp. 26–47. DOI: 10.1103/RevModPhys.41.26.

[28] H. C. Volkin. "Calculation of short-pulse propagation in a large CO_2-laser amplifier". In: *J. Appl. Phys.* 50 (1979), pp. 1179–1188. DOI: 10.1063/1.326148.

[29] W. J. Witteman. *The CO_2 Laser*. Berlin Heidelberg New York Tokyo: Springer-Verlag, 1987.